




Magneto-vortical effect in strongly coupled plasma

Yanyan Bu^{1,a}, Shu Lin^{2,b} 

¹ School of Physics, Harbin Institute of Technology, Harbin 150001, China

² School of Physics and Astronomy, Sun Yat-Sen University, Zhuhai 519082, China

Received: 14 February 2020 / Accepted: 18 April 2020 / Published online: 11 May 2020
© The Author(s) 2020

Abstract Based on a holographic model incorporating both the chiral anomaly and the gravitational anomaly, we study the effect of magneto-vortical coupling on the transport properties of a strongly coupled plasma. The focus of present work is on the generation of a vector charge density and an axial current, as response to vorticity in a magnetized plasma. The transport coefficients parameterizing the vector charge density and axial current are calculated both analytically (in the weak magnetic field limit) and also numerically (for general values of the magnetic field). We find the generation of vector charge receives both non-anomalous and anomalous contributions, with the non-anomalous contribution dominating in the limit of a strong magnetic field and the anomalous contribution sensitive to both chiral anomaly and gravitational anomaly. On the contrary, we find the axial current is induced entirely due to the gravitational anomaly, thus we interpret the axial current generation as chiral vortical effect. The corresponding chiral vortical conductivity is found to be suppressed by the magnetic field. By the Onsager relation, these transport coefficients are responsible for the generation of a thermal current due to a transverse electric field or a transverse axial magnetic field, which we call the thermal Hall effect and the thermal axial magnetic effect, respectively.

1 Introduction

The effect of magnetic field and vorticity on QCD matter has attracted much attention over the past few years. At very high temperature, when quarks become asymptotically free, a charged-neutral QCD matter can be either magnetized in the magnetic field or polarized in the vorticity field. Close to the chiral phase transition, when the interaction among quarks becomes strong, more interesting phenomena such as inverse

magnetic catalysis [1–4] and vector meson condensation [5, 6] can emerge. Similarly, the vorticity field may suppress the chiral condensation [7, 8].

When the QCD matter carries net vector charge or axial charge densities, the chiral anomaly and gravitational anomaly can induce a variety of anomalous transport phenomena such as the chiral magnetic effect (CME) [9–11], the chiral vortical effect (CVE) [12–14] and the chiral separation effect (CSE) [15, 16].

Recently, the interplay of a strong magnetic field and a vorticity was found to lead to new transport phenomena such as dynamical generation of a vector charge [17]; see also [18–21]. Under the lowest Landau level (LLL) approximation, Hattori and Yin found the generation of a vector charge from spin–vorticity coupling as [17]¹

$$J^t = q_f \frac{C_A}{2} (\vec{B} \cdot \vec{\Omega}), \quad (1)$$

with $C_A = \frac{1}{2\pi^2}$ the chiral anomaly coefficient. In fact, such a contribution should be viewed as a large B , free limit of a QED plasma. More generally, one would expect from the viewpoint of polarizable matter [22] that

$$J^t = \xi(B, T) (\vec{B} \cdot \vec{\Omega}). \quad (2)$$

Moreover, if we could associate an effective chemical potential for the generated vector charge, this can further give rise to the generation of an axial current by the chiral anomaly and gravitational anomaly. Note that the vector charge susceptibility is $\chi = C_A q_f |B|$ in the LLL approximation, and thus (1) corresponds to the effective chemical potential $\mu_{\text{eff}} = \frac{\text{sgn}(q_f)}{2} \vec{\Omega} \cdot \hat{B}$ with $\hat{B} = \vec{B}/|B|$. The vector charge imbalance would result in an axial current through the chiral

^a e-mail: yybu@hit.edu.cn

^b e-mail: linshu8@mail.sysu.edu.cn (corresponding author)

¹ See also [8] for possible contribution from orbital angular momentum and vorticity coupling.

separation effect [15, 16]

$$\vec{J}_5 = |q_f| \frac{C_A}{2} (\vec{B} \cdot \vec{\Omega}) \hat{B}. \quad (3)$$

Again, this is a large B , free limit of a QED plasma. More generally, one would expect an extra contribution from the gravitational anomaly, which always induces a temperature-dependent contribution to the axial current, even in the absence of the chiral imbalance [14, 23, 24]. Therefore, we expect the more general axial current

$$\vec{J}_5 = \sigma(B, T) \vec{\Omega}. \quad (4)$$

It is worth noting that the physical picture behind (1) and (3) is the spectral flow: a shift in the background vector gauge field leads to an opposite energy shift for right- and left-handed fermions, generating a net *axial* charge. In order for the spectral flow picture to generate vector charge, we would need an axial gauge field, whose couplings to right- and left-handed fermions differ in sign, thus leading to the same energy shift for them. In the analysis of Hattori and Yin [17], the role of the axial gauge field is played by the vorticity. Indeed, in free theory, we have $\vec{S} = \vec{J}_5$ so that we can identify \vec{A}_5 with $\vec{\Omega}$ by comparing the coupling $\vec{\Omega} \cdot \vec{S}$ with $\vec{J}_5 \cdot \vec{A}_5$. However, in an interacting theory, the “equivalence” of \vec{A}_5 with $\vec{\Omega}$ is far from obvious. First of all, even in a free theory the presence of an axial gauge field as a source poses an ambiguity in the definition of currents: consistent current and covariant current could differ by terms proportional to the axial gauge field [25]. A similar ambiguity does not exist in the case with the vorticity as a source. Secondly, in an interacting theory, the vorticity couples to the angular momentum as a whole. The separation of the spin from the total angular momentum is often ambiguous. Therefore, it is desirable to go away from the free theory limit to test the robustness of the mechanism. In this paper, we go to the opposite limit, where the theory is strongly coupled. Specifically, we will study the response of a strongly coupled magnetized plasma to the vorticity field by a holographic model.

The rest of the paper is organized as follows: In Sect. 2, we present the setup of the holographic model. In Sect. 3, we turn on a metric perturbation as a proxy for the vorticity in the magnetized plasma. We will study the response of the vector charge density and axial current to the vorticity. In Sect. 4, we will present both analytic results in the small B regime and numerical results for general B . In Sect. 5, we use the Onsager relation to obtain the thermal Hall effect and the thermal axial magnetic effect. We conclude and discuss implications of our results in Sect. 6. Details of the computations are collected in Appendices A, B and C.

2 Holographic setup: magnetic brane in AdS_5

2.1 Gravity action and dictionary

We extend the holographic model initially considered in [26, 27] by including both vector and axial gauge fields. The full action is

$$S = \frac{1}{2\kappa^2} \int d^5x \sqrt{-g} \left\{ R[g] + 12 - \frac{1}{4} (F^V)^2 - \frac{1}{4} (F^a)^2 + \epsilon^{MNPQR} A_M \times \left[\frac{1}{3} \alpha (F^a)_{NP} (F^a)_{QR} + \alpha (F^V)_{NP} (F^V)_{QR} + \lambda R^Y_{XNP} R^X_{YQR} \right] \right\} + \frac{1}{\kappa^2} \int d^4x \sqrt{-\gamma} K[\gamma] + S_{\text{CSK}} + S_{\text{c.t.}}, \quad (5)$$

where $F^V = dV$ and $F^a = dA$. The last line of (5) corresponds to boundary terms defined on the hypersurface Σ of constant r . The notation γ denotes the determinant of the induced metric $\gamma_{\mu\nu}$ on Σ :

$$ds^2|_{\Sigma} = g_{MN} dx^M dx^N|_{\Sigma} = \gamma_{\mu\nu} dx^\mu dx^\nu. \quad (6)$$

We also need the out-pointing unit normal vector of the surface Σ :

$$n_M = \frac{\partial_M r}{\sqrt{g^{AB} \partial_A r \partial_B r}}. \quad (7)$$

Moreover, $K = \gamma^{\mu\nu} K_{\mu\nu}$ whereas $K_{\mu\nu}$ is the extrinsic curvature tensor

$$K_{\mu\nu} = \frac{1}{2} \mathcal{L}_n \gamma_{\mu\nu} = \frac{1}{2} \left(n^M \partial_M \gamma_{\mu\nu} + \gamma_{\mu N} \partial_\nu n^N + \gamma_{\nu N} \partial_\mu n^N \right). \quad (8)$$

The Levi-Civita tensor is $\epsilon^{MNPQR} = \epsilon(MNPQR)/\sqrt{-g}$ whereas $\epsilon(MNPQR)$ is the Levi-Civita symbol under the convention $\epsilon(rtxyz) = +1$. The purely gauge Chern-Simons action (α -terms) mimics the chiral anomaly, while the mixed gauge-gravitational Chern-Simons term (λ -term) is to model the gravitational anomaly of the boundary field theory.

As explained in [27], in order to get a correct form of the gravitational anomaly (i.e. guarantee the gauge variation of the bulk action to be a total derivative), one needs to add the term

$$S_{\text{CSK}} = -\frac{4}{\kappa^2} \lambda \int d^4x \sqrt{-\gamma} n_M \epsilon^{MNPQR} A_N K_{PL} \tilde{\nabla}_Q K_R^L, \quad (9)$$

where $\tilde{\nabla}$ is compatible with the induced metric γ_{AB} . The counter-term action is

$$S_{\text{c.t.}} = -\frac{1}{2\kappa^2} \int d^4x \sqrt{-\gamma} \left(6 + \frac{1}{2} R[\gamma] - \mathcal{C}_t \right), \quad (10)$$

where \mathcal{C}_t cancels the logarithmic divergences [28, 29]

$$\mathcal{C}_t = \frac{1}{4} \log r \left[\left(F^V \right)_{\mu\nu} \left(F^V \right)^{\mu\nu} + \left(F^a \right)_{\mu\nu} \left(F^a \right)^{\mu\nu} \right] + \log \frac{1}{r^2} \left(\frac{1}{8} R^{\mu\nu} [\gamma] R_{\mu\nu} [\gamma] - \frac{1}{24} R^2 [\gamma] \right). \quad (11)$$

Note that \mathcal{C}_t non-vanishes only when non-trivial sources (either external gauge fields or non-flat boundary metric) are turned on for the boundary theory. In addition, in \mathcal{C}_t we employ the minimal subtraction scheme so that it will not generate *finite* contribution to the boundary currents and stress tensor.

According to the holographic dictionary, the expectation values of the stress tensor and currents of the boundary theory are defined as

$$T_{\mu\nu} \equiv \lim_{r \rightarrow \infty} \frac{-2r^2}{\sqrt{-\gamma}} \frac{\delta S}{\delta \gamma^{\mu\nu}}, \quad J^\mu \equiv \lim_{r \rightarrow \infty} \frac{\delta S}{\delta V_\mu}, \quad J_5^\mu \equiv \lim_{r \rightarrow \infty} \frac{\delta S}{\delta A_\mu}. \quad (12)$$

Explicitly, the vector current is (from now on, we set $2\kappa^2 = 1$ for convenience)

$$J^\mu = \lim_{r \rightarrow \infty} \sqrt{-\gamma} \left\{ n_M \left(F^V \right)^{\mu M} + 4\alpha n_M \epsilon^{M\mu NQR} A_N \left(F^V \right)_{QR} - \tilde{\nabla}_\nu \left(F^V \right)^{\nu\mu} \log r \right\}. \quad (13)$$

However, the axial current and stress tensor are somewhat subtle and complicated:

$$J_5^\mu = \lim_{r \rightarrow \infty} \sqrt{-\gamma} \left\{ n_M \left(F^a \right)^{\mu M} + \frac{4}{3} \alpha n_M \epsilon^{M\mu NQR} A_N \left(F^a \right)_{QR} - \tilde{\nabla}_\nu \left(F^a \right)^{\nu\mu} \log r + J_{\text{CSK}}^\mu \right\}, \quad (14)$$

$$T_{\mu\nu} = -2 \lim_{r \rightarrow \infty} r^2 \left(K_{\mu\nu} - K \gamma_{\mu\nu} + 3\gamma_{\mu\nu} - \frac{1}{2} \mathcal{G}_{\mu\nu} [\gamma] - T_{\mu\nu}^{\text{Gra}} \right) + T_{\mu\nu}^{\text{C}}, \quad (15)$$

where $T_{\mu\nu}^{\text{C}}$ arises from the functional derivative of \mathcal{C}_t , J_{CSK}^μ is due to the added action S_{CSK} , and $T_{\mu\nu}^{\text{Gra}}$ comes from the gravitational Chern–Simons term. The expressions for all of them are [27, 30]

$$J_{\text{CSK}}^\mu = -8\lambda n_M \epsilon^{M\mu PQR} K_{PL} \tilde{\nabla}_Q K_R^L, \quad T_{\mu\nu}^{\text{C}} = T_{\mu\nu}^{\text{C}_1} + \lim_{r \rightarrow \infty} \frac{1}{4} r^6 \log r \left[\gamma_{\mu\nu} (F^V)_{\alpha\beta} (F^V)^{\alpha\beta} - 4(F^V)_{\mu\alpha} (F^V)_{\nu}^{\alpha} \right] + (V \rightarrow a), \quad T_{\text{Gra}}^{\mu\nu} = 4\lambda \epsilon^{(\mu\alpha\beta\rho} \left[\frac{1}{2} (F^a)_{\alpha\beta} R_{\rho}^{\nu)} [\gamma] + \tilde{\nabla}_\delta \left(A_\alpha R_{\beta\rho}^{\delta\nu)} [\gamma] \right) \right], \quad (16)$$

where $T_{\mu\nu}^{\text{C}_1}$ vanishes for a flat boundary. $T_{\text{Gra}}^{\mu\nu}$ was first derived in [30] based on the ADM decomposition approach. Above, we stick to the consistent current formalism. Indeed, in the absence of a background for the axial gauge field, there will be no difference between the consistent current and covariant current [25]. The authors of [26] presented a thorough analysis for the holographic renormalization of the model, but did not get the term S_{CSK} . Additionally, the authors of [26] addressed the fact that the gravitational Chern–Simons term will make a contribution to the boundary stress tensor. See also [30, 31] for more recently updated formulas for stress tensor and axial current of the boundary theory. The holographic model does correctly describe the chiral/gravitational anomalies for the boundary field theory [27]:

$$\hat{\nabla}_\mu J^\mu = 0, \quad \hat{\nabla}_\mu J_5^\mu = 8\alpha \hat{\epsilon}^{\alpha\beta\rho\delta} \hat{F}_{\alpha\beta} \hat{F}_{\rho\delta} + \lambda \hat{\epsilon}^{\alpha\beta\rho\delta} \hat{R}_{\kappa\alpha\beta}^{\tau} \hat{R}_{\tau\rho\delta}^{\kappa}, \quad (17)$$

where a hat means that the corresponding quantity is defined on the boundary.

Under the variation

$$g_{MN} \rightarrow g_{MN} + \delta g_{MN}, \quad V_M \rightarrow V_M + \delta V_M, \quad A_M \rightarrow A_M + \delta A_M, \quad (18)$$

one obtains the Einstein equation

$$0 = E_{MN} \equiv R_{MN} - \frac{1}{2} R g_{MN} - 6g_{MN} - T_{MN}^{\text{bulk}}, \quad (19)$$

and anomalous Maxwell equations

$$0 = E V^M \equiv \nabla_N \left(F^V \right)^{NM} + 2\alpha \epsilon^{MNPQR} \left(F^a \right)_{NP} \left(F^V \right)_{QR}, \quad (20)$$

$$0 = E A^M \equiv \nabla_N \left(F^a \right)^{NM} + \alpha \epsilon^{MNPQR} \left[\left(F^V \right)_{NP} \left(F^V \right)_{QR} + \left(F^a \right)_{NP} \left(F^a \right)_{QR} \right] + \lambda \epsilon^{MNPQR} R_{XNP}^Y R_{YQR}^X. \quad (21)$$

The bulk stress tensor T_{MN}^{bulk} could be split into two parts,

$$T_{MN}^{\text{bulk}} = T_{MN}^{\text{Maxwell}} - \nabla_X \Theta_{MN}^X, \quad (22)$$

where

$$T_{MN}^{\text{Maxwell}} = \frac{1}{2} \left(F^V \right)_{RM} \left(F^V \right)_N^R - \frac{1}{8} g_{MN} \left(F^V \right)^2 + \frac{1}{2} \left(F^a \right)_{RM} \left(F^a \right)_N^R - \frac{1}{8} g_{MN} \left(F^a \right)^2 \quad (23)$$

$$\Theta_{MN}^X = \lambda \epsilon^{QRSTU} \left(g_{QM} R_{NRS}^X + g_{QN} R_{MRS}^X \right) \left(F^a \right)_{TU}. \quad (24)$$

Alternatively, the Einstein equation could be rewritten as

$$0 = E_{MN} = R_{MN} + 4g_{MN} - \tilde{T}_{MN}^{\text{bulk}} \quad (25)$$

where

$$\begin{aligned} \tilde{T}_{MN}^{\text{bulk}} = & \frac{1}{2}(F^V)_{RM}(F^V)_N^R - \frac{1}{12}g_{MN}(F^V)^2 \\ & + \frac{1}{2}(F^a)_{RM}(F^a)_N^R - \frac{1}{12}g_{MN}(F^a)^2 \\ & - \nabla_X \Theta_{MN}^X + \frac{1}{3}g_{MN}g^{AB}\nabla_X \Theta_{AB}^X. \end{aligned} \quad (26)$$

2.2 Neutral magnetic brane background

To proceed, we consider the background solution of the holographic model (5). For simplicity, we focus on a neutral magnetized plasma. To this end, we turn on a constant magnetic field along the z -direction,

$$V = Bx dy \Rightarrow \vec{B} = B\hat{z}, \quad (27)$$

which obviously breaks the $SO(3)$ rotational symmetry to $SO(2)_\perp$ on the xy -plane. As a result, the background metric takes the form

$$ds^2 = 2drdt - f(r)dt^2 + e^{2W_T(r)}(dx^2 + dy^2) + e^{2W_L(r)}dz^2. \quad (28)$$

Note that in writing down (28), the ingoing Eddington–Finkelstein coordinate has been employed in order to avoid a coordinate singularity. The background metric (28) has an event horizon at $r = r_h$ so that

$$f(r \simeq r_h) = 0 + f'(r_h)(r - r_h) + \dots, \quad (29)$$

while W_T, W_L are regular at $r = r_h$. The Hawking temperature, identified as the temperature of the dual gauge theory, is

$$T = \left. \frac{\partial_r(f(r))}{4\pi} \right|_{r=r_h}. \quad (30)$$

Generically, both $W_T(r)$ and $W_L(r)$ will depend on r_h non-trivially.

It is a simple exercise to check that, given the above ansatz (27) and (28), both the gauge and the gravitational Chern–Simons terms do not affect the bulk equations of motion. Therefore, the background geometry is simply the “magnetic brane” solution initially studied in [32].

The ordinary differential equations (ODEs) for the metric functions in (28) are

$$E_{rr} = 0 : \quad 0 = W_L'^2 + 2W_T'^2 + W_L'' + 2W_T'', \quad (31)$$

$$\begin{aligned} E_{rt} = 0 = E_{tt} : \quad & 24 + B^2 e^{-4W_T(r)} \\ & = 3f'(W_L' + 2W_T') + 3f'', \end{aligned} \quad (32)$$

$$\begin{aligned} E_{xx} = 0 = E_{yy} : \quad & 12 - B^2 e^{-4W_T(r)} \\ & = 3f'W_T' + 3f(W_L'W_T' + 2W_T'^2 + W_T''), \end{aligned} \quad (33)$$

$$\begin{aligned} E_{zz} = 0 : \quad & 24 + B^2 e^{-4W_T(r)} \\ & = 6f'W_L' + 6f(W_L'^2 + 2W_L'W_T' + W_L''), \end{aligned} \quad (34)$$

where the prime denotes a derivative with respect to r . Equations (33) and (34) look different from those of [32]. However, suitable combinations of the above equations give rise to the results of [32]:

$$\begin{aligned} 2 \times (33) - (34) & \Rightarrow 2f(W_T'' - W_L'') + 2[f' + f(W_L' + 2W_T')] \\ & (W_T' - W_L') = -B^2 e^{-4W_T(r)}, \\ 4 \times (33) + (34) & \Rightarrow 2f'(2W_T' + W_L') + 4fW_T'(W_T' + 2W_L') \\ & = 24 - B^2 e^{-4W_T(r)}. \end{aligned} \quad (35)$$

Obviously, not all the equations in (31)–(34) are independent: we will take (31) as the constraint and solve the remaining ones to determine the metric functions $f(r)$, $W_T(r)$, $W_L(r)$.

In order to fully determine $f(r)$, $W_T(r)$, $W_L(r)$, we have to impose two boundary conditions for each of them. For $f(r)$, we impose

$$f(r = r_h) = 0; \quad \underline{f(r \rightarrow \infty) \rightarrow r^2}. \quad (36)$$

However, it is found that the second boundary condition (underlined above) is automatically satisfied by the bulk EOMs. This requires one to impose another condition for $f(r)$, which is explained in Appendix 1. For $W_T(r)$ and $W_L(r)$, the boundary conditions are

$$W_T(r), W_L(r) \rightarrow \log r, \quad \text{as } r \rightarrow \infty, \quad (37)$$

$$12 - B^2 e^{-4W_T(r)} = 3f'W_T', \quad \text{at } r = r_h, \quad (38)$$

$$24 + B^2 e^{-4W_T(r)} = 6f'W_L', \quad \text{at } r = r_h, \quad (39)$$

where the last two equations are read off from (33) and (34) by requiring regularity of $W_T(r)$, $W_L(r)$ at the horizon $r = r_h$.

We solve the bulk EOMs (31)–(34) analytically when the magnetic field is weak (i.e., $B/T^2 \ll 1$) and numerically when B is general. The calculational details as well as the main results are deferred to Appendix A.

3 Fluctuation in the bulk theory: general consideration

3.1 Bulk perturbations

In this section, we study the linear response of the magnetized plasma to a fluid vorticity. A weak fluid vorticity $\vec{\Omega}$ would be mimicked by a gravito-magnetic field [27, 31]. More precisely, one perturbs the boundary Minkowski space-time (where the fluid flows) as

$$ds_M^2 = -dt^2 + d\vec{x}^2 + 2h_{ti}(t, \vec{x})dt dx^i, \quad (40)$$

with $h_{ti}(t, \vec{x}) = u_i(t, \vec{x})$.

Then the vorticity is generated at linear order in h_{ti} as

$$\Omega^i = \frac{1}{2}\epsilon^{ijk}\nabla_j u_k = \frac{1}{2}\epsilon^{ijk}\partial_j h_{tk}, \quad (41)$$

with the unperturbed fluid velocity $u^\mu = (1, 0, 0, 0)$. Thus, the curl of h_{ti} could be thought of as a fluid vorticity. We take

$$h_{ti}(\vec{x}) = e^{iqx} h_{ty}(q) \delta_{yi}, \quad (42)$$

which gives rise to a stationary vorticity along the z -direction, i.e. parallel to the magnetic field. Then we can obtain the Kubo formulas for the transport coefficients defined in (2) and (4) as

$$\xi = \frac{2}{B} \lim_{q \rightarrow 0} \frac{\langle J^t T^{ty} \rangle}{iq}, \quad \sigma = 2 \lim_{q \rightarrow 0} \frac{\langle J_5^z T^{ty} \rangle}{iq}. \quad (43)$$

These will be used in holographic calculations.

To turn on a gravito-magnetic field in the bulk, it is convenient to use the Poincaré coordinate system so that the bulk metric takes a diagonal form,

$$ds^2 = -f(r)dt^2 + \frac{dr^2}{f(r)} + e^{2W_T(r)} \times (dx^2 + dy^2) + e^{2W_L(r)} dz^2, \quad (44)$$

where we still denote the time of the bulk theory by t . On top of the background (44) and (27), it is consistent to turn on the following fluctuation modes:

$$\begin{aligned} \delta(ds^2) &= 2e^{W_T(r)} [\delta g_{ty}(r, t, x) dt dy + \delta g_{xy}(r, t, x) dx dy], \\ \delta V &= \delta V_t(r, t, x) dt + \delta V_x(r, t, x) dx, \\ \delta A &= \delta A_z(r, t, x) dz, \end{aligned} \quad (45)$$

while setting all the rest corrections to zero. Here, we have assumed (t, x) -dependent fluctuations for a reason to be discussed in the next subsection and we consider a plane wave ansatz:

$$\begin{aligned} \delta g_{ty}(r, t, x) &\sim e^{-i\omega t + iqx} \delta g_{ty}(r), \\ \delta g_{xy}(r, t, x) &\sim e^{-i\omega t + iqx} \delta g_{xy}(r), \\ \delta V_t(r, t, x) &\sim e^{-i\omega t + iqx} \delta V_t(r), \\ \delta V_x(r, t, x) &\sim e^{-i\omega t + iqx} \delta V_x(r), \\ \delta A_z(r, t, x) &\sim e^{-i\omega t + iqx} \delta A_z(r). \end{aligned} \quad (46)$$

In what follows we record the bulk equations of motion for the fluctuation modes. First, we consider the constraint equations. The constraint $E_{ry} = 0$ is

$$\begin{aligned} 0 &= \lambda \omega q e^{-W_L} \delta A_z \left(-\frac{2B^2 e^{-4W_T}}{f} + \frac{2f' W_L'}{f} \right. \\ &\quad \left. + \frac{4f' W_T'}{f} - 4W_L' W_T' - 8W_T'^2 \right) \\ &\quad + \frac{1}{2} i q \partial_r \delta g_{xy} + \frac{i \omega e^{2W_T}}{2f} \partial_r \delta g_{ty} + \frac{1}{2} B e^{-2W_T} \partial_r \delta V_x. \end{aligned} \quad (47)$$

The constraint $E V^r = 0$ gives

$$0 = 8\omega \alpha B \delta A_z + q e^{W_L} f \partial_r \delta V_x + \omega e^{W_L + 2W_T} \partial_r \delta V_t. \quad (48)$$

Next, we turn to the dynamical components of the bulk EOMs. The Einstein equation $E_{ty} = 0$ reads

$$\begin{aligned} 0 &= \partial_r \left(e^{W_L + 4W_T} \partial_r \delta g_{ty} \right) - \frac{B^2 e^{W_L}}{f(r)} \delta g_{ty} - \frac{q^2 e^{W_L + 2W_T}}{f(r)} \delta g_{ty} \\ &\quad - \frac{\omega q e^{W_L + 2W_T}}{f} \delta g_{xy} + \frac{i \omega B e^{W_L}}{f} \delta V_x \\ &\quad + \frac{i q B e^{W_L}}{f(r)} \delta V_t + i q \lambda e^{2W_T} \partial_r \delta A_z \\ &\quad \times \left(4B^2 e^{-4W_T} - 4f' W_L' - 8f' W_T' \right. \\ &\quad \left. + 8f W_T' W_L' + 16f W_T'^2 \right) + i q \lambda e^{2W_T} \delta A_z \\ &\quad \times \left(2B^2 e^{-4W_T} f^{-1} f' - 48f^{-1} f' - 4B^2 e^{-4W_T} W_L' \right. \\ &\quad \left. + 4f^{-1} f'^2 W_L' + 8f' W_L'^2 - 20B^2 e^{-4W_T} W_T' \right. \\ &\quad \left. + 96W_T' + 8f^{-1} f'^2 W_T' + 16f' W_T' W_L' \right. \\ &\quad \left. - 16f W_T' W_L'^2 - 48f W_L' W_T'^2 - 32f W_T'^3 \right). \end{aligned} \quad (49)$$

The Einstein equation $E_{xy} = 0$ is

$$\begin{aligned} 0 &= \partial_r \left(e^{W_L + 2W_T} f \partial_r \delta g_{xy} \right) + \frac{\omega^2 e^{W_L + 2W_T}}{f} \delta g_{xy} \\ &\quad + \frac{\omega q e^{W_L + 2W_T}}{f} \delta g_{ty}. \end{aligned} \quad (50)$$

The Maxwell equation $E V^t = 0$ is

$$\begin{aligned} 0 &= \partial_r \left(e^{W_L + 2W_T} \partial_r \delta V_t \right) + 8\alpha B \partial_r \delta A_z - \frac{\omega q e^{W_L}}{f} \delta V_x \\ &\quad - \frac{q^2 e^{W_L}}{f} \delta V_t - \frac{i q B e^{W_L}}{f} \delta g_{ty}. \end{aligned} \quad (51)$$

The Maxwell equation $EV^x = 0$ is

$$0 = \partial_r \left(e^{W_L} f \partial_r \delta V_x \right) + \frac{\omega^2 e^{W_L}}{f} \delta V_x + \frac{\omega q e^{W_L}}{f} \delta V_t + \frac{i \omega B e^{W_L}}{f} \delta g_{ty}. \quad (52)$$

Finally, $EA^z = 0$ yields

$$0 = \partial_r \left(e^{2W_T - W_L} f \partial_r \delta A_z \right) + \frac{\omega^2 e^{2W_T - W_L}}{f} \delta A_z - q^2 e^{-W_L} \delta A_z + i q \lambda e^{2W_T} \left(-4B^2 e^{-4W_T} + 4f' W_L' \right. \\ \left. + 8f' W_T' - 8f W_T' W_L' - 16f W_T'^2 \right) \partial_r \delta g_{ty} + 8\alpha B \partial_r \delta V_t. \quad (53)$$

3.2 Adiabatic limit and boundary conditions

From the Kubo formulas (43), it seems as if we could set $\omega = 0$ from the beginning. However, the boundary condition at the horizon cannot be uniquely determined in this case. This ambiguity is related to the ambiguity in the Kubo formula itself. It can be evaluated in any equilibrium state, be it charged or neutral. For our purpose, it should be evaluated in the unperturbed neutral plasma state. The boundary condition to use should correspond to the neutral state. In practice, we specify the state as follows: the state is realized by turning on the vorticity field adiabatically to the original neutral magnetized plasma.

We will seek solutions to (47) through (53) in the adiabatic limit $\omega \rightarrow 0$. To this end, we expand the bulk perturbations in powers of ω :

$$X = X^{(0)} + \omega X^{(1)} + \dots, \quad (54)$$

with $X = \delta g_{xy}, \delta V_x, \delta g_{ty}, \delta V_t$ and δA_z . In fact, we only need the leading order solution $X^{(0)}$, for which we suppress the superscript (0). The fields decouple into two sets $\{\delta g_{xy}, \delta V_x\}$ and $\{\delta g_{ty}, \delta V_t, \delta A_z\}$. The set $\{\delta g_{ty}, \delta V_t, \delta A_z\}$ satisfies the following equations:

$$\partial_r \left(e^{W_L + 4W_T} \partial_r \delta g_{ty} \right) - \frac{B^2 e^{W_L}}{f(r)} \delta g_{ty} - \frac{q^2 e^{W_L + 2W_T}}{f(r)} \delta g_{ty} + \frac{i q B e^{W_L}}{f(r)} \delta V_t + i q \lambda e^{2W_T} \partial_r \delta A_z \\ \times \left(4B^2 e^{-4W_T} - 4f' W_L' - 8f' W_T' \right. \\ \left. + 8f W_T' W_L' + 16f W_T'^2 \right) \\ + i q \lambda e^{2W_T} \delta A_z \left(2B^2 e^{-4W_T} f^{-1} f' - 48f^{-1} f' \right. \\ \left. - 4B^2 e^{-4W_T} W_L' + 4f^{-1} f'^2 W_L' \right. \\ \left. + 8f' W_L'^2 - 20B^2 e^{-4W_T} + 96W_T' + 8f^{-1} f'^2 W_T' \right. \\ \left. + 16f' W_T' W_L' - 16f W_T' W_L'^2 \right. \\ \left. - 48f W_L' W_T'^2 - 32f W_T'^3 \right) = 0, \quad (55)$$

$$\partial_r \left(e^{W_L + 2W_T} \partial_r \delta V_t \right) + 8\alpha B \partial_r \delta A_z - \frac{q^2 e^{W_L}}{f} \delta V_t - \frac{i q B e^{W_L}}{f} \delta g_{ty} = 0, \quad (56)$$

$$\partial_r \left(e^{2W_T - W_L} f \partial_r \delta A_z \right) - q^2 e^{-W_L} \delta A_z + i q \lambda e^{2W_T} \left(-4B^2 e^{-4W_T} + 4f' W_L' + 8f' W_T' \right. \\ \left. - 8f W_T' W_L' - 16f W_T'^2 \right) \partial_r \delta g_{ty} + 8\alpha B \partial_r \delta V_t = 0. \quad (57)$$

The boundary conditions on the horizon need to be derived by matching with the horizon solutions in the limit $\omega \rightarrow 0$. We elaborate on the derivation in Appendix B. The resultant boundary conditions on the horizon are given by

$$\delta g_{ty}(r = r_h) = 0, \quad \delta V_t(r = r_h) = 0, \\ \delta A_z(r = r_h) = \text{constant}. \quad (58)$$

The free parameters for the three fields can be chosen as horizon derivatives of $\delta g_{ty}, \delta V_t$ and horizon value of δA_z . The three parameters on the horizon can be mapped to boundary values of the three fields. We can further simplify Eqs. (55)–(57) by considering the limit $q \rightarrow 0$. Note that δg_{ty} has an opposite parity to those of δV_t and δA_z , and δg_{ty} is the only field sourced on the AdS boundary. Therefore, the AdS boundary conditions are

$$\delta g_{ty} \xrightarrow{r \rightarrow \infty} h_{ty}, \quad \text{others} \xrightarrow{r \rightarrow \infty} 0. \quad (59)$$

We expect the scaling behaviors $\delta g_{ty} \sim \mathcal{O}(q^0)$, and $\delta V_t, \delta A_z \sim \mathcal{O}(q)$. Defining $\delta V_t = i q \delta \tilde{V}_t$ and $\delta A_z = i q \delta \tilde{A}_z$, we can further simplify (55) through (57) by keeping the leading terms in the q -expansion

$$\partial_r \left(e^{W_L + 4W_T} \partial_r \delta g_{ty} \right) - \frac{B^2 e^{W_L}}{f(r)} \delta g_{ty} = 0, \\ \partial_r \left(e^{W_L + 2W_T} \partial_r \delta \tilde{V}_t \right) + 8\alpha B \partial_r \delta \tilde{A}_z - \frac{B e^{W_L}}{f} \delta g_{ty} = 0, \\ \partial_r \left(e^{2W_T - W_L} f \partial_r \delta \tilde{A}_z \right) + \lambda e^{2W_T} \left(-4B^2 e^{-4W_T} + 4f' W_L' \right. \\ \left. + 8f' W_T' - 8f W_T' W_L' - 16f W_T'^2 \right) \partial_r \delta g_{ty} + 8\alpha B \partial_r \delta \tilde{V}_t = 0. \quad (60)$$

4 The correlators $\langle J^t T^{ty} \rangle$ and $\langle J_z^z T^{ty} \rangle$

In this section, we calculate the generation of J^t and J_z^z as linear responses to the external source h_{ty} . Note that h_{ty} couples

to T^{ty} in the boundary theory. We can express the responses in terms of retarded correlators $\langle J^t T^{ty} \rangle$ and $\langle J_5^z T^{ty} \rangle$ as

$$\begin{aligned} J^t(\omega, q) &= \langle J^t(\omega, q) T^{ty}(-\omega, -q) \rangle h_{ty}(\omega, q), \\ J_5^z(\omega, q) &= \langle J_5^z(\omega, q) T^{ty}(-\omega, -q) \rangle h_{ty}(\omega, q), \end{aligned} \quad (61)$$

with the retarded correlators defined as

$$\begin{aligned} \langle J^t(\omega, q) T^{ty}(-\omega, -q) \rangle &= \int \frac{dt d^3x}{(2\pi)^4} (-i) e^{-i\omega t + i\vec{q} \cdot \vec{x}} \theta(t) \langle [J^t(t, x), T^{ty}(0)] \rangle, \\ \langle J_5^z(\omega, q) T^{ty}(-\omega, -q) \rangle &= \int \frac{dt d^3x}{(2\pi)^4} (-i) e^{-i\omega t + i\vec{q} \cdot \vec{x}} \theta(t) \langle [J_5^z(t, x), T^{ty}(0)] \rangle. \end{aligned} \quad (62)$$

Equation (61) relates the above retarded correlators in equilibrium to the responses of J^t and J_5^z to h_{ty} , which are exactly the quantities we will calculate. So, instead of directly computing the retarded correlators (62), we will read off them by computing the one-point functions of J^t and J_5^z (with the only source h_{ty} turned on).

The bulk EOMs (60) will be solved under the boundary conditions (58) and (59). This section will be further split into two parts: an analytical study when the magnetic field is weak versus a numerical study when the value of the magnetic field is generic. In these two complementary studies, we will utilize the results of the background metric functions summarized in Appendix A.

In the limit $\omega \rightarrow 0$ and $q \rightarrow 0$, the vector charge density and the axial current are (in terms of the bulk fields)

$$\begin{aligned} J^t &= \lim_{r \rightarrow \infty} \left\{ e^{W_L + 2W_T} \partial_r \delta V_t - \frac{e^{W_L}}{\sqrt{f(r)}} (B \partial_x \delta g_{ty}) \log r \right\}, \\ J_5^z &= \lim_{r \rightarrow \infty} \left\{ -f(r) e^{2W_T - W_L} \partial_r \delta A_z \right\}. \end{aligned} \quad (63)$$

Near the AdS boundary, the bulk fluctuations behave as

$$\begin{aligned} \delta g_{ty} &\xrightarrow{r \rightarrow \infty} h_{ty} + \frac{B^2 h_{ty}}{4r^4} \log \frac{r_h}{r} + \frac{t_{ty}}{r^4} + \mathcal{O}(r^{-5}), \\ \delta \tilde{V}_t &\xrightarrow{r \rightarrow \infty} \frac{B h_{ty}}{2r^2} \log \frac{r_h}{r} + \frac{v_t^2}{r^2} + \mathcal{O}(r^{-3} \log r), \\ \delta \tilde{A}_z &\xrightarrow{r \rightarrow \infty} \frac{a_z^2}{r^2} + \mathcal{O}(r^{-3}). \end{aligned} \quad (64)$$

So, the vector charge density and axial current for the boundary theory are

$$J^t = -2v_t^2 i q - B i q h_{ty} \left(\log r_h + \frac{1}{2} \right), \quad J_5^z = 2i q a_z^2. \quad (65)$$

Below we solve for J^t and J_5^z perturbatively in B and also numerically for generic B .

4.1 Weak magnetic field: a perturbative study

When the magnetic field B is weak, the bulk fluctuations are expandable,

$$\begin{aligned} \delta g_{ty} &= \delta g_{ty}^{[0]} + \epsilon^2 \delta g_{ty}^{[2]} + \dots, \\ \delta \tilde{V}_t &= \epsilon \delta \tilde{V}_t^{[1]} + \epsilon^3 \delta \tilde{V}_t^{[3]} + \dots, \\ \delta \tilde{A}_z &= \delta \tilde{A}_z^{[0]} + \epsilon^2 \delta \tilde{A}_z^{[2]} + \dots, \end{aligned} \quad (66)$$

where $\epsilon \sim B$. At the lowest order $\mathcal{O}(\epsilon^0)$, first we have

$$0 = \partial_r \left(r^5 \partial_r \delta g_{ty}^{[0]} \right) \implies \delta g_{ty}^{[0]} = \left(1 - \frac{r_h^4}{r^4} \right) h_{ty}. \quad (67)$$

Then we have

$$0 = \partial_r \left((r^3 - r_h^4/r) \partial_r \delta \tilde{A}_z^{[0]} \right) + \frac{48\lambda r_h^4}{r^2} \partial_r \delta g_{ty}^{[0]}, \quad (68)$$

whose solution is

$$\delta \tilde{A}_z^{[0]} = 8\lambda \left(\frac{r_h^4}{r^4} + 2 \log \frac{r^2 + r_h^2}{r^2} \right) h_{ty}. \quad (69)$$

At the first order $\mathcal{O}(\epsilon^1)$,

$$0 = \partial_r \left(r^3 \partial_r \delta \tilde{V}_t^{[1]} \right) + 8\alpha B \partial_r \delta \tilde{A}_z^{[0]} - \frac{B}{r} h_{ty}, \quad (70)$$

which is solved by

$$\begin{aligned} \delta \tilde{V}_t^{[1]} &= B h_{ty} \left\{ \frac{\log(r_h/r)}{2r^2} - \frac{128(\log 2)\alpha\lambda}{r^2} + \frac{32\alpha\lambda}{3r^6} (r_h^4 - r^4) \right. \\ &\quad \left. + 64\alpha\lambda \left(\frac{1}{r^2} + \frac{1}{r_h^2} \right) \log \frac{r^2 + r_h^2}{r^2} \right\} \\ &\xrightarrow{r \rightarrow \infty} \left\{ -\frac{\log r}{2r^2} + \frac{1}{r^2} \left(\frac{1}{2} \log r_h + \frac{160}{3} \alpha\lambda \right. \right. \\ &\quad \left. \left. - 128 \log 2 \alpha\lambda \right) \right\} B h_{ty} + \mathcal{O}(r^{-3}). \end{aligned} \quad (71)$$

At the second order $\mathcal{O}(\epsilon^2)$:

$$0 = \partial_r \left(r^5 \partial_r \delta g_{ty}^{[2]} \right) - \frac{B^2}{r} h_{ty} + 8r_h^4 W_T^{(2)'}(r) h_{ty}. \quad (72)$$

Here, we would like to recall that $W_T^{(2)}$ is obtained in (114). The solution for $\delta g_{ty}^{[2]}$ would be

$$\delta g_{ty}^{[2]}(r) = -B^2 h_{ty} \int_r^\infty \frac{\log x}{x^5} dx$$

$$+ 8r_h^4 h_{ty} \int_r^\infty \frac{W_T^{(2)}(x)}{x^5} dx + \frac{C}{r^4}, \quad (73)$$

where the integration constant C is fixed as

$$\begin{aligned} \delta g_{ty}^{[2]}(r = r_h) = 0 &\implies C = B^2 r_h^4 h_{ty} \int_{r_h}^\infty \frac{\log x}{x^5} dx \\ &\quad - 8r_h^8 h_{ty} \int_{r_h}^\infty \frac{W_T^{(2)}(x)}{x^5} dx \\ &= \frac{1}{24} B^2 h_{ty} (1 + 6 \log r_h). \end{aligned} \quad (74)$$

So,

$$\begin{aligned} \partial_r \delta g_{ty}^{[2]}(r) = h_{ty} &\left\{ \frac{B^2 \log r}{r^5} - \frac{8r_h^4}{r^5} W_T^{(2)}(r) \right. \\ &\quad \left. - \frac{1}{6r^5} B^2 (1 + 6 \log r_h) \right\}. \end{aligned} \quad (75)$$

The equation for $\delta \tilde{A}_z^{[2]}$ is

$$\begin{aligned} 0 = \partial_r \left[(r^3 - r_h^4/r) \partial_r \delta \tilde{A}_z^{[2]} \right] &+ \alpha H_1(r) \\ &+ \alpha^2 \lambda H_2(r) + \lambda H_3(r), \end{aligned} \quad (76)$$

where

$$\begin{aligned} H_1(r) &= h_{ty} \left(-\frac{4B^2}{r^3} - \frac{8B^2 \log(r_h/r)}{r^3} \right), \\ H_2(r) &= h_{ty} \left[-\frac{512B^2 r_h^4}{r^7} + \frac{512B^2 (12 \log 2 - 5)}{3r^3} \right. \\ &\quad \left. - \frac{1024B^2}{r^3} \log \left(1 + \frac{r_h^2}{r^2} \right) \right], \\ H_3(r) &= h_{ty} \left\{ -\frac{80B^2 r_h^4}{3r^7} + \frac{16B^2 r_h^2}{3r^3 (r^2 + r_h^2)} \right. \\ &\quad + \frac{64r_h^2 (r_h^4 - r_p^4)}{r (r^2 + r_h^2)} \left(\frac{1}{r^2 + r_h^2} + \frac{1}{r^2} \right) \\ &\quad + \left[\frac{32B^2 r_h^2}{3r (r^2 + r_h^2)^2} + \frac{32B^2 r_h^2}{3r^3 (r^2 + r_h^2)} - \frac{48B^2 r_h^4}{r^7} \right] \\ &\quad \log \frac{r_h}{r} - \frac{768r_h^8 W_T^{(2)}}{r^7} \\ &\quad \left. + 32r_h^2 W_T^{(2)} \left[\frac{7r_h^2 (r_h^6 - r^6)}{r^6} + \frac{4(r_h^4 - r^4)}{r^2 (r^2 + r_h^2)} \right] \right\}. \end{aligned} \quad (77)$$

The solution and the near-boundary expansion for $\delta \tilde{A}_z^{[2]}$ are

$$\begin{aligned} \delta \tilde{A}_z^{[2]}(r) &= \int_r^\infty \frac{dx}{x^3 - r_h^4/x} \\ &\quad \times \int_{r_h}^x \left[\alpha H_1(y) + \alpha^2 \lambda H_2(y) + \lambda H_3(y) \right] dy \\ &\xrightarrow{r \rightarrow \infty} -\frac{4\lambda h_{ty} (B^2 - 6r_h^4 + 6r_p^4)}{3r_h^2 r^2} + \mathcal{O}(r^{-3}). \end{aligned} \quad (78)$$

Up to $\mathcal{O}(B^2)$, the vector charge density and axial current on the boundary are

$$\begin{aligned} J^t &= \left[\frac{64}{3} (12 \log 2 - 5) \alpha \lambda - \log r_h - \frac{1}{2} \right] B i q h_{ty} + \dots, \\ J_5^z &= 32\lambda r_h^2 i q h_{ty} - \frac{8\lambda}{3r_h^2} (B^2 - 6r_h^4 + 6r_p^4) i q h_{ty} + \dots. \end{aligned} \quad (79)$$

The transport coefficients ξ and σ are

$$\begin{aligned} \xi &= \frac{128}{3} (12 \log 2 - 5) \alpha \lambda - 2 \log r_h - 1 + \mathcal{O}(B/T^2), \\ \sigma &= r_h^2 \left[64\lambda - \frac{32\lambda B}{3r_h^2} + \mathcal{O}(B^2/T^4) \right], \end{aligned} \quad (80)$$

where we have substituted the perturbative expression (116) for r_p .

The transport coefficient ξ contains both non-anomalous contribution and anomalous contribution proportional to $\alpha\lambda$. The non-anomalous contribution is consistent with the prediction of the non-anomalous magnetohydrodynamics (MHD) [33], which for a neutral plasma has²

$$\Delta J^t = 2 \left(M_{\Omega, \mu} \vec{B} \cdot \vec{\Omega} - 2p_{,B^2} \vec{B} \cdot \vec{\Omega} \right), \quad (81)$$

with $M_\Omega \equiv \frac{\partial \mathcal{F}}{\partial (B \cdot \Omega)}$ being the magneto-vortical susceptibility and $2p_{,B^2} \equiv 2 \frac{\partial p}{\partial (B^2)}$ being the magnetic susceptibility. Here p is the pressure and \mathcal{F} is the free energy density [33]. Note that in (81) we ignored terms nonlinear in Ω . Both susceptibilities M_Ω and $2p_{,B^2}$ can be calculated independently. In the weak B field limit, the magnetic susceptibility $2p_{,B^2}$ can be calculated from the perturbative background we already obtain in Appendix A. While the magneto-vortical susceptibility M_Ω vanishes for a neutral plasma by charge conjugation symmetry, $M_{\Omega, \mu} \equiv \partial M_\Omega / \partial \mu$ does not. The quantity $M_{\Omega, \mu}$ can even be calculated in a charged plasma at $B = 0$.

² In comparison with [33], we have included an overall factor 2 given that the fluid's vorticity defined in (41) is half of that of [33].

In Appendix C, we calculate both susceptibilities with the following results:

$$2p_{,B^2} = \log r_h, \quad M_{\Omega,\mu} = -\frac{1}{2}. \quad (82)$$

The negative value of $M_{\Omega,\mu}$ is consistent with the fact that spin-vorticity coupling lowers/raises energy of particle/anti-particle. Clearly, (81) and (82) are in perfect agreement with (79).

The dependence $\log r_h$ may look odd at the first sight. To restore units, we should use the replacement $\log r_h \rightarrow \log(r_h L)$. In fact, this transport coefficient is scheme dependent. The appearance of the AdS radius L comes from the fact that we use $1/L$ as our renormalization scale [34]. Other physically significant renormalization scales could be used, which could alter this term [34]. It is also interesting to note that the scheme dependence is related conformal anomaly. In fact, a different scheme would correspond to adding a finite counter-term as

$$\Delta S_{\text{c.t.}} = -\frac{1}{2\kappa^2} \int d^4x \sqrt{-\gamma} \left(\frac{a}{4} (F^V)_{\mu\nu} (F^V)^{\mu\nu} \right). \quad (83)$$

Such a counter-term would give the following contribution to the vector current:

$$\Delta J^\mu = -\frac{a}{2\kappa^2} \sqrt{-\gamma} \nabla_\nu F^{\mu\nu}. \quad (84)$$

In the presence of $h_{ty}(x)$, we can easily obtain $\Delta J^t \sim a \vec{B} \cdot \vec{\Omega}$. Therefore the combination $M_{\Omega,\mu} - 2p_{,B^2}$ can be shifted by a constant. Note that the scheme dependence of the vector charge density is absent in a free theory.

The anomalous contribution is proportional to $\lambda\alpha B$. The EOM (60) suggests the following chain of responses: $\delta A_z \sim \mathcal{O}(\lambda)$ is induced in response to vorticity and then backreaction of δA_z to δV^t gives $J^t \sim \mathcal{O}(\lambda\alpha B)$. This corresponds to the backreaction of J_5^z generated by CVE to J^t on the field theory side. A possible $\alpha^2 B^2$ -term would emerge at the next order $\mathcal{O}(B^2)$. In this case, (60) suggests the following chain of responses: a non-anomalous contribution to J^t is generated by magneto-vortical coupling. Then J_5^z is induced by CSE. The backreaction of J_5^z to J^t would give the $\mathcal{O}(\alpha^2 B^2)$ contribution. However, the above reasoning is not quite accurate. As we show below, in fact CSE is not generated in the presence of J^t . Nevertheless the bulk profile of δA_z does backreact to δV_t to give $\alpha^2 B^2$ correction to J^t .

In contrast to ξ , the transport coefficient σ is scheme independent. We can add an analogous counter-term as (83). It would not contribute to J_5^z in the absence of a background axial gauge field. The structure of σ is relatively simple. Aside from the T^2 -correction to the CVE (i.e., the first piece in σ), σ encodes the correction to chiral vortical coefficient from B . However, there is no contribution proportional to α .

In other words, no CSE is seen despite the generation of J^t . This is in contrast to the naive expectation from CSE

$$J_5^z = 8\alpha B \frac{J^t}{\chi}, \quad (85)$$

with χ being the vector charge susceptibility. In fact, from the holographic model, the absence of CSE holds more generally: if we integrate (57) from the horizon to an arbitrary r , we obtain (with $\lambda = 0$)

$$e^{2W_T - W_L} f \partial_r \delta \tilde{A}_z + 8\alpha B \delta \tilde{V}_t(r) = 0, \quad (86)$$

where the horizon boundary conditions (58) have been utilized to fix the integration constant. Taking $r \rightarrow \infty$ and noting $\tilde{V}_t(r \rightarrow \infty) = 0$, we have

$$J_5^z = 0, \quad \text{when } \lambda = 0. \quad (87)$$

Following [35], we should identify the difference of δV_t on the boundary and on the horizon as the vector chemical potential

$$\mu = \delta V_t(r = \infty) - \delta V_t(r = r_h). \quad (88)$$

It then follows naturally from (86) that $J_5^z = 8\alpha B\mu$. In our case, we have $\mu = 0$ but $J^t \neq 0$.

To understand the physical difference between J^t and μ , we note μ ($-\mu$) is the extra energy cost to create one unit of particle (anti-particle), but J^t depends on actual distribution of particles and anti-particles. In our case $\mu = 0$ implies that it costs the same energy to create both particle and anti-particle. Indeed, we can view δV_t as a zero mode as it vanishes both on the horizon and on the boundary, which supports the picture of vanishing energy cost for creating a particle. Since the state is obtained by the adiabatic limit, it means J^t is generated dynamically³. The CSE seems to be only sensitive to the energy difference μ , not the charge density. The absence of CSE can also be understood from the scheme independence J_5^z : unlike J^t , J_5^z is unaffected by the choice of scheme from (63). This makes natural for J_5^z to depend on μ , rather than on J^t .

4.2 Generic magnetic field: a numerical study

For generic values of B , we will solve the fluctuation EOMs (60) through the shooting technique. First, we find the near-horizon solution:

³ Interestingly, similar situations have been found for the equilibrium state [36,37].

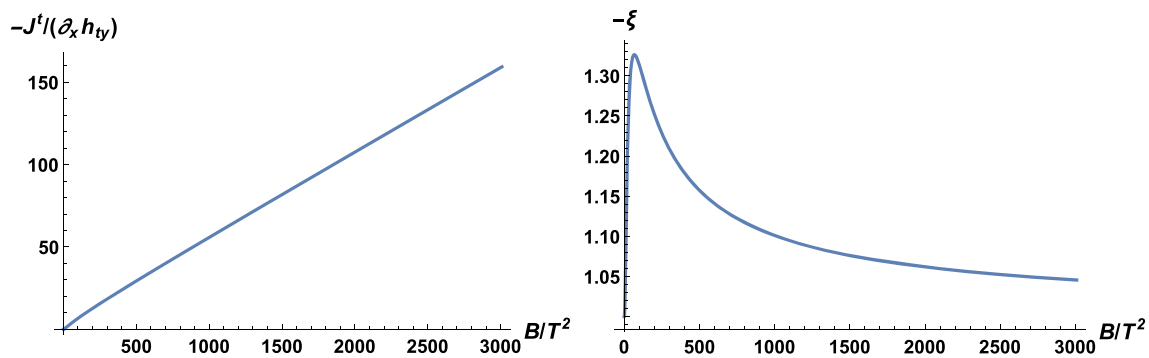


Fig. 1 The correlator $\langle J^t T^{ty} \rangle / (iq) = J^t / \partial_x h_{ty}$ in units of r_h^2 (left) and the transport coefficient ξ (right) as a function of B/T^2 when $\alpha = \lambda = 0$

$$\begin{aligned} \delta g_{ty} &= \delta g_{ty}^1 (r - r_h) + \delta g_{ty}^2 (r - r_h)^2 + \dots, \\ \delta \tilde{V}_t &= \delta \tilde{V}_t^1 (r - r_h) + \delta \tilde{V}_t^2 (r - r_h)^2 + \dots, \\ \delta \tilde{A}_z &= \delta \tilde{A}_z^0 + \delta \tilde{A}_z^1 (r - r_h) + \delta \tilde{A}_z^2 (r - r_h)^2 + \dots, \end{aligned} \quad (89)$$

where, thanks to the horizon condition (58), only δg_{ty}^1 , $\delta \tilde{V}_t^1$ and $\delta \tilde{A}_z^0$ are undetermined. Then we will choose a reasonable value of δg_{ty}^1 (this corresponds to turning on a specific source h_{ty}) and fine-tune $\delta \tilde{V}_t^1$, $\delta \tilde{A}_z^0$ until $\delta \tilde{V}_t(r = \infty) = \delta \tilde{A}_z(r = \infty) = 0$ are satisfied. From the numerical solution, we can read off the expectation values of J^t and J_5^z , as responses to the source h_{ty} only. In practical numerics, we set the horizon data $\delta g_{ty}^1 = -1$.

However, there is one problem in the procedure mentioned above. Since we intend to solve the background EOMs (32)–(34) using the initial conditions (122) and (124), we should be careful in solving the fluctuation EOMs (60). More precisely, the correct solutions are

$$\delta g_{ty} = \frac{\delta g_{ty}^*}{\sqrt{v(b)}}, \quad \delta V_t = \delta V_t^*, \quad \delta A_z = \frac{\delta A_z^*}{\sqrt{w(b)}}, \quad (90)$$

where the starred functions δg_{ty}^* , δV_t^* and δA_z^* are solved from (60) using the “incorrect” numerical background metric functions, as discussed in Appendix A. Adapted to the tilde variables, we have

$$\begin{aligned} \frac{\delta \tilde{V}_t}{B} &= \frac{\delta V_t}{iqB} = v^{3/2}(b) \delta \tilde{V}_t^*, \\ \tilde{A}_z &\equiv \frac{\delta A_z}{iq} = \sqrt{\frac{v(b)}{w(b)}} \delta \tilde{A}_z^*. \end{aligned} \quad (91)$$

Here, for the sake of numerical calculation, we have further re-scaled the term $\delta \tilde{V}_t$ of (60) by a factor of B .

For convenience, we set $r_h = 1$ in our numerical calculations. So, the dimensionful quantities (J^t , J_5^z etc.) to be plotted in Sects. 4.2.1 and 4.2.2 should be understood as in units of proper powers of r_h .

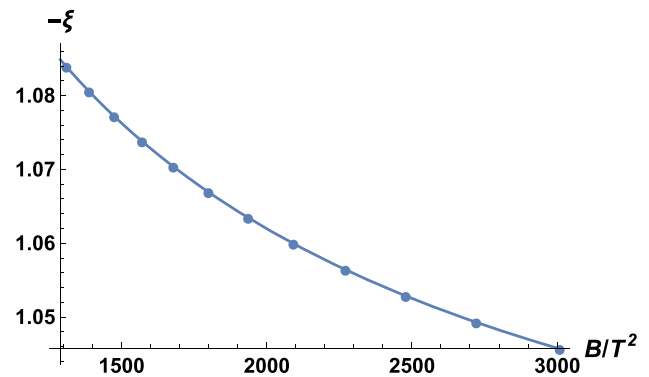


Fig. 2 In the strong B limit, the numerical result of ξ (dots) is fitted by the function (92) when $\alpha = \lambda = 0$

4.2.1 Non-anomalous effects: $\alpha = \lambda = 0$

When the chiral anomaly and gravitational anomaly are turned off (i.e., $\alpha = \lambda = 0$), the transport properties of the magnetized plasma get non-anomalous contributions from the medium only. The medium effects are not covered by the study of [17] since the calculations therein are essentially based on the vacuum state. In this situation, as we discussed in the previous section we only see a dynamically generated vector charge density J^t , whereas the correlator $\langle J_5^z T^{ty} \rangle / (iq)$ (and thus J_5^z) vanishes identically as seen from (87). In Fig. 1, we show the correlator $\langle J^t T^{ty} \rangle / (iq)$ and the transport coefficient ξ as a function of B/T^2 . For the purpose of probing the strong magnetic field limit, we have improved our numerical calculations and generate plots up to $B/T^2 \sim 3000$.

From the left panel of Fig. 1, it *seemingly* implies a quasi-linear growth for $\langle J^t T^{ty} \rangle / (iq)$ as B/T^2 is increased, which as we will show is inaccurate. The right panel of Fig. 1 reveals more information: $-\xi$ approaches 1 from above. In Fig. 2, we fit our numerical result for ξ in the strong magnetic field limit by the following function:

$$-\xi \simeq 1.0001779 + 32.692107 \frac{\log(B/T^2)}{B/T^2} + \frac{124.89109}{B/T^2}. \quad (92)$$

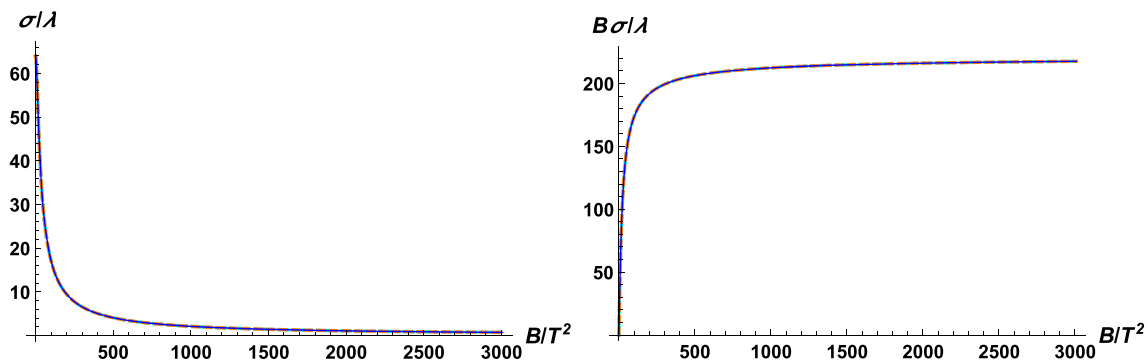


Fig. 3 Left: the CVE conductivity σ in units of r_h^2 (with anomaly coefficient λ factorized out) as a function of B/T^2 . Right: $B\sigma/\lambda$ in unit of r_h^4 , demonstrating the asymptotic behavior for σ at strong magnetic field.

Here, in each plot the three curves (dashed orange, solid blue, dotted green) corresponding to the different choice in (93) perfectly collapse into a single one

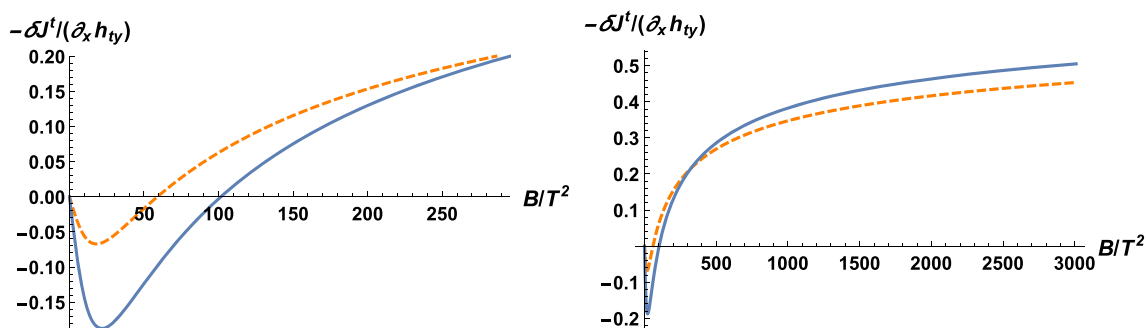


Fig. 4 The anomalous correction $\langle \delta J^t T^{ty} \rangle / (iq)$ in unit of r_h^2 as a function of B/T^2 : $\alpha = 1/20$, $\lambda = 1/50$ for dashed curve and $\alpha = 1/20$, $\lambda = 1/20$ for solid one

It is tempting to conclude that $-\xi \rightarrow 1$ asymptotically. The correction in (92) can be understood as the v_t^2 term in the general expression (65) by noting that $r_h = 1$ in our numerical results.

4.2.2 Anomalous effects: $\lambda \neq 0$

We now turn attention to the anomalous contributions to the transport properties of the magnetized plasma. While the two anomaly coefficients, α , λ , are fixed for a specific QFT on the boundary, we here take a phenomenological viewpoint and think of α , λ as free parameters. First of all, taking $\lambda = 0$ will kill J_5^z completely, as seen from the bulk EOMs (60). Thus, our representative choices for the anomaly coefficients are

$$(\alpha, \lambda) = (0, 1/50), (1/20, 1/50), (1/20, 1/20). \quad (93)$$

We begin with the fate of the CVE conductivity σ . First, the last equation of (60) could be formally integrated from the horizon to the AdS boundary, yielding

$$J_5^z = \sigma \Omega + 8\alpha \mu B, \quad (94)$$

where μ is defined in (88). Here, we stress that the CVE conductivity σ depends on λ linearly and is independent of α . In the left panel of Fig. 3, we plot the CVE conductivity σ as a function of B/T^2 , taking all choices for α , λ from (93). From the plot, we obviously see perfect overlapping of different curves, confirming our claim that σ linearly depends on λ only. Intriguingly, the magneto-vortical coupling effect tends to suppress the CVE conductivity and eventually renders it vanishing at large magnetic field. Asymptotically, $\sigma \sim B^{-1}$ as demonstrated in the right panel of Fig. 3. Similar suppression effects due to the quark mass [38, 39] and spacetime curvature [40] are seen. Our findings are in contrast to the proposal of [17] that the magneto-vortical coupling (through the chiral anomaly) generates a term to σ linear in B when B/T^2 becomes very large.

Next, we consider anomalous contributions to the generation of the vector charge density J^t and the transport coefficient ξ . Given that J^t always gets a non-anomalous contribution, we find it more transparent to consider

$$\delta J^t \equiv J^t - J^t|_{\alpha=\lambda=0}, \quad \delta \xi \equiv \xi - \xi|_{\alpha=\lambda=0}. \quad (95)$$

In accord with the different choices for α , λ as made in (93), we show anomalous corrections $\langle \delta J^t T^{ty} \rangle / (iq)$ and $\delta \xi$ in

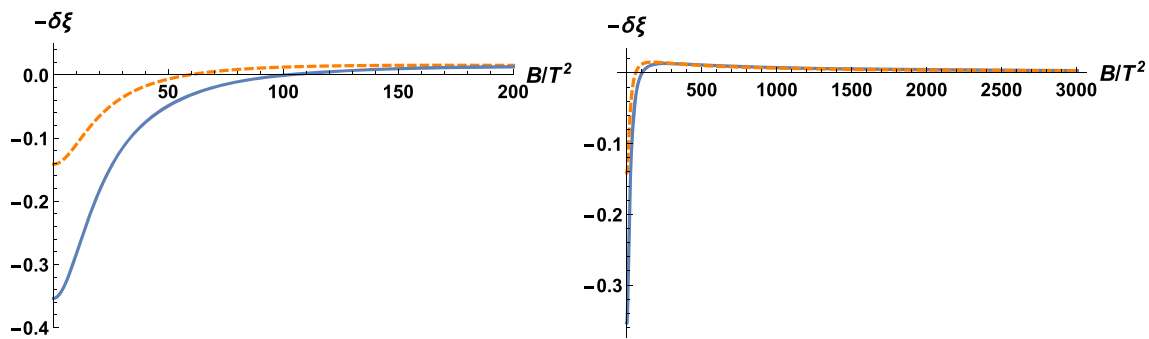


Fig. 5 The anomalous correction $\delta\xi$ as a function of B/T^2 : $\alpha = 1/20$, $\lambda = 1/50$ for the dashed curve and $\alpha = 1/20$, $\lambda = 1/20$ for the solid one

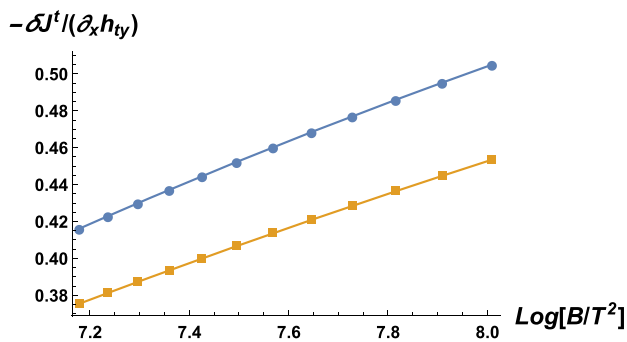


Fig. 6 The anomalous correction $\langle \delta J^t T^{ty} \rangle / (iq)$ in unit of r_h^2 as a function of $\log(B/T^2)$: $\alpha = 1/20$, $\lambda = 1/50$ for the squared points and $\alpha = 1/20$, $\lambda = 1/20$ for the circled points

Figs. 4 and 5, respectively. From the second equation of (60), it is clear that taking $\alpha = 0$ makes anomalous contributions δJ^t and $\delta\xi$ to be zero. So, for each panel of Figs. 4 and 5, we have only two non-trivial curves.

From Fig. 4, we read that the anomalous contribution to the vector charge δJ^t has opposite sign to their non-anomalous counterpart for a weak magnetic field. As the magnetic field becomes stronger, δJ^t changes sign and continues to grow mildly at large B/T^2 . More precisely, the numerical results at large B imply the following asymptotic behaviors for the anomalous corrections:

$$\delta J^t \simeq \log B, \quad \delta\xi \simeq \frac{\log B}{B}, \quad (96)$$

which are clearly confirmed by the plots of Fig. 6. It is worth noting that from (92) and (96) the large B limit of ξ is dominated by the non-anomalous medium contribution.

5 Thermal Hall effect and thermal axial magnetic effect

In the previous section, we have obtained the following transport coefficients:

$$\begin{aligned} J^t &= \xi(B, T)(\vec{B} \cdot \vec{\Omega}), \\ J_5^z &= \sigma(B, T)\Omega, \end{aligned} \quad (97)$$

which can be viewed as responses of J^t and J_5^z to h_{ty} (cf. (61)):

$$\begin{aligned} J^t(q) &= \langle J^t(q) T^{ty}(-q) \rangle_B h_{ty}(q) = \frac{iq\xi(B, T)B}{2} h_{ty}(q), \\ J_5^z(q) &= \langle J_5^z(q) T^{ty}(-q) \rangle_B h_{ty}(q) = \frac{iq\sigma(B, T)}{2} h_{ty}(q), \end{aligned} \quad (98)$$

where we have substituted the expression for Ω in (41). The correlators in (98) give the following transposed correlators by the Onsager relation:

$$\begin{aligned} \langle T^{ty}(-q) J^t(q) \rangle_{-B} &= \frac{1}{2} iq\xi(B, T)B, \\ \langle T^{ty}(-q) J_5^z(q) \rangle_{-B} &= \frac{1}{2} iq\sigma(B, T). \end{aligned} \quad (99)$$

The subscript indicates the expectation values are taken with $-B$. We can then obtain the response of T^{ty} to both A_t and A_z^5 using (99) with the signs of both q and B flipped

$$\begin{aligned} T^{ty}(q) &= \langle T^{ty}(q) J^t(-q) \rangle_B A_t(q) = \frac{1}{2} \xi(-B, T) E_x(q) B, \\ T^{ty}(q) &= \langle T^{ty}(q) J_5^z(-q) \rangle_B A_z^5(q) = \frac{1}{2} \sigma(-B, T) B_{5y}(q), \end{aligned} \quad (100)$$

where we have used $E_x(q) = -iqA_t(q)$ and $B_{5y}(q) = -iqA_z^5(q)$. In a neutral plasma, (100) corresponds to the generation of thermal current by transverse electric field and transverse axial magnetic field, which we coin the thermal Hall effect and the thermal axial magnetic effect, respectively. Below we will derive (100) more rigorously using the time-reversal symmetry. We start with the following correlators for the responses to h_{ty} :

$$\langle J^t(q) T^{ty}(-q) \rangle = \frac{iq\xi B}{2},$$

$$\langle J_5^z(q) T^{ty}(-q) \rangle = \frac{iq\sigma}{2}, \quad (101)$$

with the correlators in (101) being the limit $\omega \rightarrow 0$ of the following retarded correlator:

$$\begin{aligned} \langle O_a(\omega, q) O_b(-\omega, -q) \rangle &= \int \frac{dt d^3x}{(2\pi)^4} e^{-i\omega t + i\vec{q} \cdot \vec{x}} G_{ab}^R(t, x, B) \\ &= \int \frac{dt d^3x}{(2\pi)^4} (-i) e^{-i\omega t + i\vec{q} \cdot \vec{x}} \theta(t) \langle [O_a(t, x), O_b(0)] \rangle. \end{aligned} \quad (102)$$

By time-reversal symmetry, we can obtain the transposed correlators by [41]

$$\begin{aligned} G_{ab}^R(t, x, B) &= \gamma_a \gamma_b G_{ba}^R(t, -x, -B) \\ &\Rightarrow \langle O_a(\omega, q) O_b(-\omega, -q) \rangle_B \\ &= \gamma_a \gamma_b \langle O_b(\omega, -q) O_a(-\omega, q) \rangle_{-B} \end{aligned} \quad (103)$$

with $\gamma_a = \pm 1$ corresponding to eigenvalues of operator O_a under time-reversal. Note that B flips sign under time-reversal, which we indicate in the subscript. For the operators of our interest T^{ty} , J^t , J_5^z , we have $\gamma = -, +, +$, respectively. Therefore, (101) and (103) give the following transposed correlators (with the direction of B reversed and $\omega = 0$):

$$\begin{aligned} \langle T^{ty}(-q) J^t(q) \rangle_{-B} &= -\frac{1}{2} iq \xi(B) B, \\ \langle T^{ty}(-q) J_5^z(q) \rangle_{-B} &= -\frac{1}{2} iq \sigma(B). \end{aligned} \quad (104)$$

Note that $J^t(q)$ and $J_5^z(q)$ couple to sources $V_t(-q)$ and $A_z(-q)$, respectively. We can rewrite (104) in a more intuitive way:

$$\begin{aligned} \langle T^{ty}(-q) \rangle_{-B} &= \frac{1}{2} \xi(B) B E_x(-q), \\ \langle T^{ty}(-q) \rangle_{-B} &= \frac{1}{2} \sigma(B) B v_y(-q). \end{aligned} \quad (105)$$

The thermal Hall effect contains both non-anomalous and anomalous contributions, where the non-anomalous contribution can be understood from non-anomalous MHD [33]. Naively, turning on E_x necessarily induces a steady flow along v_y due to the Lorentz force acting on positive and negative charge carriers. However, this is not true for a stationary state. The stationary state can be obtained simply by setting $\omega = 0$ in (47) through (53). In this case, the dynamics of the fields δg_{ty} , δV_t , δA_z decouple from δV_x , δg_{xy} . We can thus consistently set δV_x and δg_{xy} to zero, leading to vanishing J^x and T^{xy} . This strongly constrains the hydrodynamic analysis. Note that both J^x and T^{xy} contain the dissipative terms as follows:

$$\begin{aligned} J^x &= \sigma (E_x - \partial_x \mu + v_y B), \\ T^{xy} &= \eta \partial_x v_y + \dots \end{aligned}$$

The shear contribution in T^{xy} cannot be canceled by other terms. The only possibility for T^{xy} to vanish is to have $v_y = 0$. This implies that an inhomogeneous vector charge density is needed for the stationary state: $E_x - \partial_x \mu = 0$. Indeed, this is consistent with the holographic analysis if we identify $\mu = V_t(r = \infty) - V_t(r = r_h)$. With $v_y = 0$, the non-anomalous contribution to the thermal current is given by [33, 42–44])

$$T^{ty} = -E_x B (2p_{B^2} - M_{\Omega, \mu}). \quad (106)$$

The first term can be identified as $-E_x M$ by noting $2p_{B^2} B = M$. The second term can be interpreted as $-P_x B$ if we identify $E_x M_{\Omega, \mu}$ as an effective polarization P_x . Apart from the non-anomalous contribution, we also obtain an anomalous contribution that requires at least the chiral anomaly to exist. This can be seen from the middle equation in (60). When $\alpha = 0$, the dynamics of δA_z decouples from that of δV_t , leaving only a non-anomalous contribution. On the contrary, the thermal axial magnetic effect contains only an anomalous effect. Its existence relies on the gravitational anomaly.

6 Conclusion

In this work, based on a holographic model, we considered the effects of the magneto-vortical coupling on the transport properties of a strongly coupled plasma. First of all, even when the chiral and gravitational anomalies are turned off, the coupling of a magnetic field and a weak fluid's vorticity dynamically generate a contribution to the vector charge density J^t , which we refer to as a non-anomalous medium contribution. The non-anomalous medium contribution in J^t grows linearly in B and the relevant transport ξ approaches a constant in the strong magnetic field limit. However, a similar non-anomalous contribution is not observed for the axial current.

Secondly, the magneto-vortical coupling also generates anomalous contributions to the vector charge density J^t and axial current J_5^z . Thanks to the absence of a background for the vector chemical potential, the anomalous contribution to J_5^z is completely induced by the gravitational anomaly (i.e., insensitive to the chiral anomaly). In this sense, it would be more natural to interpret the anomalous contribution to J_5^z as a CVE contribution [27], rather than a CSE contribution. The corresponding chiral vortical conductivity receives a correction at finite B . In particular, in the strong magnetic field limit, the magneto-vortical coupling renders the CVE conductivity vanishing asymptotically. This is quantitatively different

from the conclusion of [17]. In contrast to that of J_5^z , the anomalous contribution to J^I requires the chiral anomaly to exist. The presence of a gravitational anomaly can also affect the generation of J^I . Thus, the anomalous contribution to J^I would contain more fruitful physics. Particularly, in the strong magnetic field limit, the anomalous part of J^I seemingly grows logarithmically as a function of B . This is to be compared with the results of [17] where a term linear in B was generated in J^I by the chiral anomaly.

Our findings summarized above would necessitate the formulating of a consistent/complete anomalous magnetohydrodynamics. This requires one to consistently add novel transport phenomena induced by anomalies into the non-anomalous magnetohydrodynamics [33, 42]. While our study treated the magnetic field as external, the case with a dynamical electromagnetic field is also interesting. The corresponding anomalous MHD has been initially considered in [45] by assuming a small chiral anomaly coefficient. In fact, holographic models corresponding to a dynamical electromagnetic field have been proposed in [46, 47]. Including anomalies in the model would allow us to study anomalous MHD without further assumptions on the anomaly coefficients. We leave this for future work.

Last but not least, the transport phenomena we discussed are dissipationless. It is possible to derive them by including anomalies in the partition function approach [48]. This would allow us to obtain more complete dissipationless transport phenomena. We hope to address this in the future.

Acknowledgements We would like to thank K. Hattori, J.F. Liao, K. Mameda, R.X. Miao, I. Shovkovy, H.-U. Yee and Y. Yin for useful discussions related to this work. YB was supported by the Fundamental Research Funds for the Central Universities under grant No.122050205032 and the Natural Science Foundation of China (NSFC) under the grant No.11705037. SL was supported by the NSFC under the grant Nos. 11675274 and 11735007. SL also thanks Yukawa Institute of Theoretical Physics for hospitality and the workshop “Quantum kinetic theories in magnetic and vortical fields” for providing a stimulating environment during the final stage of this work.

Data Availability Statement This manuscript has no associated data or the data will not be deposited. [Authors’ comment: This is a theoretical study and no experimental data has been listed.]

Open Access This article is licensed under a Creative Commons Attribution 4.0 International License, which permits use, sharing, adaptation, distribution and reproduction in any medium or format, as long as you give appropriate credit to the original author(s) and the source, provide a link to the Creative Commons licence, and indicate if changes were made. The images or other third party material in this article are included in the article’s Creative Commons licence, unless indicated otherwise in a credit line to the material. If material is not included in the article’s Creative Commons licence and your intended use is not permitted by statutory regulation or exceeds the permitted use, you will need to obtain permission directly from the copyright holder. To view a copy of this licence, visit <http://creativecommons.org/licenses/by/4.0/>. Funded by SCOAP³.

Appendix A: Details of solving the background metric functions

In this appendix, we collect calculational details of solving the background metric functions.

When the magnetic field is weak (i.e. $B/T^2 \ll 1$), we construct the bulk metric functions perturbatively [49]:

$$\begin{aligned} f(r) &= r^2 - \frac{r_h^4}{r^2} + \epsilon^2 f^{(2)}(r) + \epsilon^4 f^{(4)}(r) + \dots, \\ W_T(r) &= \log r + \epsilon^2 W_T^{(2)}(r) + \epsilon^4 W_T^{(4)}(r) + \dots, \\ W_L(r) &= \log r + \epsilon^2 W_L^{(2)}(r) + \epsilon^4 W_L^{(4)}(r) + \dots, \end{aligned} \quad (107)$$

where a formal parameter $\epsilon \sim B/T^2$ is introduced to mark the perturbative expansion. $f^{(n)}(r)$, $W_T^{(n)}(r)$ and $W_L^{(n)}(r)$ are solved from the bulk equations. We are interested in $n = 2$.

At $\mathcal{O}(\epsilon^2)$, the constraint equation (31) yields

$$W_L^{(2)} + 2W_T^{(2)} = c_1 + \frac{c_2}{r}, \quad (108)$$

where the integration constant c_1 should be set to zero due to asymptotic AdS requirement (37). By redefinition of the radial coordinate r , we could also set $c_2 = 0$. Thus,

$$W_L^{(2)} + 2W_T^{(2)} = 0. \quad (109)$$

Then the dynamical equation (32) is solved as

$$\begin{aligned} r^3 \partial_r^2 f^{(2)} + 3r^2 \partial_r f^{(2)} \\ = \frac{B^2}{3r} \Rightarrow f^{(2)} = c_f^1 + \frac{c_f^2}{r^2} - \frac{B^2 \log r}{6r^2}. \end{aligned} \quad (110)$$

Substituting (109) and (110) into the dynamical equations (33) and (34), we obtain

$$\begin{aligned} 0 &= (r^5 - rr_h^4) W_T^{(2)''}(r) + (5r^4 - r_h^4) W_T^{(2)'}(r) + \frac{B^2}{6r} + 2c_f^1 r, \\ 0 &= (r^5 - rr_h^4) W_L^{(2)''}(r) + (5r^4 - r_h^4) W_L^{(2)'}(r) - \frac{B^2}{3r} + 2c_f^1 r. \end{aligned} \quad (111)$$

Obviously, in order to be consistent with (109), one has to set $c_f^1 = 0$. The integration constant c_f^2 is fixed by the location of the horizon, which will be presumably shifted due to the presence of a magnetic field,

$$\begin{aligned} \left(r^2 - \frac{r_h^4}{r^2} + f^{(2)}(r) \right) \Big|_{r=r_p^{(2)}} = 0 \Rightarrow c_f^2 \\ = - \left((r_p^{(2)})^4 - r_h^4 \right) + \frac{B^2 \log r_p^{(2)}}{6(r_p^{(2)})^2}, \end{aligned} \quad (112)$$

where $r_p^{(2)}$ represents the location of the event horizon at $\mathcal{O}(\epsilon^2)$. Then

$$f^{(2)} = -\frac{(r_p^{(2)})^4 - r_h^4}{r^2} + \frac{B^2}{6r^2} \log \frac{r_p^{(2)}}{r}. \quad (113)$$

From (33), $W_T^{(2)}$ is solved as

$$\begin{aligned} \partial_r \left[r(r^4 - r_h^4) \partial_r W_T^{(2)}(r) \right] + \frac{B^2}{6r} &= 0 \\ \Rightarrow W_T^{(2)} &= \frac{B^2}{6} \int_r^\infty \frac{\log(x/r_h)}{x(x^4 - r_h^4)} dx \\ &= \frac{B^2}{6} \int_r^\infty \frac{\log(x/r_p^{(2)})}{x(x^4 - (r_p^{(2)})^4)} dx \\ &= \frac{B^2}{288r_h^4} \left\{ \pi^2 - 24 \log^2 \frac{r_h}{r} \log \left(1 - \frac{r_h^4}{r^4} \right) \right. \\ &\quad \left. + 12i\pi \log \frac{r}{r_h} - 3\text{Li}_2 \left(\frac{r^4}{r_h^4} \right) \right\}, \end{aligned} \quad (114)$$

where in the last equality of the second line we have made use of the fact that the difference between $r_p^{(2)}$ and r_h is of $\mathcal{O}(B^2)$. At $\mathcal{O}(\epsilon^2)$, the relation between the location of the event horizon and the Hawking temperature becomes

$$r_p^{(2)} - \frac{B^2}{24(r_p^{(2)})^3} + \mathcal{O}(B^4) = \pi T, \quad (115)$$

which is solved as

$$r_p^{(2)} = r_h + \frac{B^2}{24r_h^3} + \mathcal{O}(B^4), \quad \text{with } r_h = \pi T. \quad (116)$$

When the value of B is generic, we have to solve the metric functions numerically. We find it more convenient to make the change of variables

$$\begin{aligned} f(r) &\rightarrow r^2 U(r), \quad W_T(r) \rightarrow \log r + \frac{1}{2} \log V(r), \\ W_L(r) &\rightarrow \log r + \frac{1}{2} \log W(r), \end{aligned} \quad (117)$$

followed by

$$u = \frac{r_h}{r} \in [0, 1]. \quad (118)$$

Then the dynamical bulk equations (32)–(34) turn into

$$\begin{aligned} 0 &= U''(u) + U'(u) \left(\frac{V'(u)}{V(u)} + \frac{W'(u)}{2W(u)} - \frac{5}{u} \right) \\ &\quad + U(u) \left(\frac{8}{u^2} - \frac{2V'(u)}{uV(u)} - \frac{W'(u)}{uW(u)} \right) \end{aligned}$$

$$\begin{aligned} & - \frac{B^2 u^2}{3V(u)^2} - \frac{8}{u^2}, \\ 0 &= V''(u) + V'(u) \left(\frac{U'(u)}{U(u)} + \frac{W'(u)}{2W(u)} - \frac{5}{u} \right) \\ &\quad + V(u) \left(-\frac{8}{u^2 U(u)} + \frac{8}{u^2} - \frac{2U'(u)}{uU(u)} \right. \\ &\quad \left. - \frac{W'(u)}{uW(u)} \right) + \frac{2B^2 u^2}{3U(u)V(u)}, \\ 0 &= W''(u) + W'(u) \left(\frac{U'(u)}{U(u)} + \frac{V'(u)}{V(u)} - \frac{4}{u} \right) \\ &\quad - \frac{W'(u)^2}{2W(u)} + W(u) \left(-\frac{B^2 u^2}{3V(u)^2} - \frac{8}{u^2} \right. \\ &\quad \left. + \frac{8}{u^2} - \frac{2U'(u)}{uU(u)} - \frac{2V'(u)}{uV(u)} \right), \end{aligned} \quad (119)$$

where, since we have set $r_h = 1$ above, B should be understood as B/r_h^2 .

Near the AdS boundary $u = 0$, the metric functions U, V, W are expanded as

$$\begin{aligned} U(u \rightarrow 0) &= 1 + U_b^1 u + \frac{1}{4} (U_b^1)^2 u^2 \\ &\quad + \frac{B^2}{6(V_b^0)^2} u^4 \log u + U_b^4 u^4 + \dots, \\ V(u \rightarrow 0) &= V_b^0 + V_b^0 U_b^1 u + \frac{1}{4} V_b^0 (U_b^1)^2 u^2 \\ &\quad - \frac{B^2}{12V_b^0} u^4 \log u + V_b^4 u^4 + \dots, \\ W(u \rightarrow 0) &= W_b^0 + W_b^0 U_b^1 u + \frac{1}{4} W_b^0 (U_b^1)^2 u^2 \\ &\quad + \frac{W_b^0 B^2}{6(V_b^0)^2} u^4 \log u + W_b^4 u^4 \dots, \end{aligned} \quad (120)$$

where we have made use of the constraint equation (31). Obviously, the asymptotic boundary conditions only give rise to “two” effective requirements! The regularity requirements will yield another three conditions. Just as in the fixing of c_2 , we can utilize the freedom of redefining the radial coordinate u and set $U_b^1 = 0$.

To summarize, the boundary conditions at $u = 0$ (the AdS boundary) are

$$U'(u = 0) = 0, \quad V(u = 0) = W(u = 0) = 1, \quad (121)$$

while at the event horizon $u = 1$

$$\begin{aligned} U(u = 1) &= 0, \\ U'(1)V'(1) - 8V(1) - 2U'(1)V(1) + \frac{2B^2}{3V(1)} &= 0, \end{aligned}$$

$$U'(1)W'(1) - 2W(1)U'(1) - 8W(1) - \frac{B^2W(1)}{3V(1)^2} = 0. \quad (122)$$

To find the numeric solutions, one can proceed in two different ways. The first approach would be to directly solve (119) under the boundary conditions (121) and (122). A second approach would be to replace the boundary conditions (121) by the following conditions at the horizon:

$$\begin{aligned} U(u \rightarrow 1) &= 0 + U_h^1(u-1) + U_h^2(u-1)^2 + \dots, \\ V(u \rightarrow 1) &= V_h^0 + V_h^1(u-1) + \dots, \\ W(u \rightarrow 1) &= W_h^0 + W_h^1(u-1) + \dots, \end{aligned} \quad (123)$$

where

$$U_h^1 = -4, \quad V_h^0 = 1, \quad W_h^0 = 1. \quad (124)$$

Note that the choice of U_h^1 will set $\pi T = 1$. However, solving (119) under the initial conditions (122) and (124), near the boundary $u = 0$ the solution will behave as

$$\begin{aligned} U(u \rightarrow 0) &\rightarrow 1, \quad V(u \rightarrow 0) \rightarrow v(b), \\ W(u \rightarrow 0) &\rightarrow w(b). \end{aligned} \quad (125)$$

Then the correct solution would be obtained by a further rescaling of the boundary coordinates,

$$x \rightarrow \sqrt{v(b)}x, \quad y \rightarrow \sqrt{v(b)}y, \quad z \rightarrow \sqrt{w(b)}z. \quad (126)$$

Due to the “incorrect” asymptotic boundary behavior (125), we have relabeled the magnetic field by b in (125) and (126). When solving the EOMs (119) under the initial conditions (122) and (124), the same relabeling should be made. Recalling the definition of the magnetic field $F^V = bdx \wedge dy$, the physical magnetic field B (in units of r_h^2) should be

$$B = \frac{b}{v(b)}. \quad (127)$$

Finally, we would like to point out that the background solution obtained with conditions (122) and (124) does not necessarily satisfy $U_b^1 = 0$ (cf. (120)).

Appendix B: Horizon boundary conditions from matching

We first seek solutions to (47) through (53) near the horizon with ingoing boundary conditions. We obtain the following series solutions:

$$\delta A_z = a_0(r - r_h)^\beta + a_1(r - r_h)^{\beta+1} + \dots,$$

$$\begin{aligned} \delta V_x &= b_0(r - r_h)^\beta + b_1(r - r_h)^{\beta+1} + \dots, \\ \delta g_{ty} &= c_1(r - r_h)^{\beta+1} + c_2(r - r_h)^{\beta+2} + \dots, \\ \delta V_t &= d_1(r - r_h)^{\beta+1} + d_2(r - r_h)^{\beta+2} + \dots, \\ \delta g_{xy} &= e_0(r - r_h)^\beta + e_1(r - r_h)^{\beta+1} + \dots, \end{aligned} \quad (128)$$

with $\beta = -\frac{i\omega}{f'(r_h)}$. Here, a_0 , b_0 and e_0 are free parameters, while all the rest coefficients are completely determined by them. For instance, c_1 and d_1 are

$$\begin{aligned} c_1 &= \frac{if'(r_h)}{f'(r_h) - i\omega} \\ &\times \left\{ -iB e^{-4W_T(r_h)} b_0 - 4\lambda B^2 e^{-W_L(r_h) - 6W_T(r_h)} q a_0 \right. \\ &\quad \left. + e^{-W_L(r_h) - 2W_T(r_h)} q \right. \\ &\quad \left. \times \left[e^{W_L(r_h)} e_0 + 4\lambda f'(r_h) (W'_L(r_h) + 2W'_T(r_h)) a_0 \right] \right\}, \\ d_1 &= \frac{if'(r_h)}{f'(r_h) - i\omega} e^{-W_L(r_h) - 2W_T(r_h)} \left[e^{W_L(r_h)} q b_0 + 8iB\alpha a_0 \right]. \end{aligned} \quad (129)$$

The three parameters a_0 , b_0 and e_0 do not match the five sources to the fields δA_z , δV_x , δg_{ty} , δV_t and δg_{xy} . The remaining two parameters come from pure gauge solutions, which are by gauge transformation of the trivial solution

$$\begin{aligned} \delta V_x &= -BC_1, \quad \delta g_{ty} = -i\omega C_1, \quad \delta g_{xy} = iqC_1, \\ \text{others} &= 0; \\ \delta V_t &= -i\omega C_2, \quad \delta V_x = iqC_2, \quad \text{others} = 0. \end{aligned} \quad (130)$$

The horizon solutions are to be matched with the lowest order solutions in (54) near the horizon region. Since the horizon solutions also contain δV_x and δg_{xy} , we also need the lowest order solutions to them. To the lowest order in ω , the EOMs of δV_x and δg_{xy} decouple:

$$\begin{aligned} \frac{1}{2}iq\partial_r\delta g_{xy} + \frac{1}{2}Be^{-2W_T}\partial_r\delta V_x &= 0, \\ \partial_r \left(e^{W_L + 2W_T} f \partial_r \delta g_{xy} \right) &= 0, \\ \partial_r \left(e^{W_L} f \partial_r \delta V_x \right) &= 0. \end{aligned} \quad (131)$$

They are clearly solved by constant solutions. Matching with the horizon solutions, we simply have

$$\delta V_x = b_0, \quad \delta g_{xy} = e_0. \quad (132)$$

Note that we can set the above two solutions to zero by adding pure gauge solutions. In the limit $\omega \rightarrow 0$, the pure gauge solutions do not change the horizon values of δg_{ty} , δV_t and δA_z :

$$\delta g_{ty}(r = r_h) = 0, \quad \delta V_t(r = r_h) = 0,$$

$$\delta A_z(r = r_h) = \text{constant}. \quad (133)$$

The $\omega \rightarrow 0$ limit of (129) determines the horizon derivative of δg_{ty} and δV_t . For the decoupled EOMs (55) through (57), we can take the horizon derivatives of δg_{ty} and δV_t , and horizon value of δA_z as free parameters.

Appendix C: Magnetic and magneto-vortical susceptibilities

In this appendix, we calculate the magnetic susceptibility $2p_{B^2}$ and magneto-vortical susceptibility M_Ω independently as a confirmation to our claim in (82).

Let us begin with the magnetic susceptibility $2p_{B^2}$ and the magnetization M . For the equilibrium state (corresponding to the magnetic brane background), the stress tensor for the boundary theory is computed as

$$\begin{aligned} T^{tt} &= \lim_{r \rightarrow \infty} \left\{ -2r^6 \left[-\frac{3}{f(r)} + \frac{W'_L + 2W'_T}{\sqrt{f(r)}} - \frac{B^2 e^{-4W_T} r^6 \log r}{2f(r)} \right] \right\}, \\ T^{xx} = T^{yy} &= \lim_{r \rightarrow \infty} \left\{ -2r^6 \left[3e^{-2W_T} - \frac{e^{-2W_T} f'(r)}{2\sqrt{f(r)}} \right. \right. \\ &\quad \left. \left. - \sqrt{f(r)} e^{-2W_T} (W'_L + W'_T) \right] - \frac{1}{2} B^2 e^{-6W_T} r^6 \log r \right\}, \\ T^{zz} &= \lim_{r \rightarrow \infty} \left\{ -2r^6 \left[3e^{-2W_L} - \frac{e^{-2W_L} f'(r)}{2\sqrt{f(r)}} - 2e^{-2W_L} \sqrt{f(r)} W'_T \right] \right. \\ &\quad \left. + \frac{1}{2} B^2 e^{-2W_L - 4W_T} r^6 \log r \right\}. \end{aligned} \quad (134)$$

With the analytical solution presented in Appendix A, it is straightforward to compute the various components of $T^{\mu\nu}$:

$$\begin{aligned} T^{tt} &= 3r_h^4 + 3(r_p^4 - r_h^4) - \frac{1}{2} B^2 \log r_h + \mathcal{O}(B^3), \\ T^{xx} = T^{yy} &= r_h^4 + (r_p^4 - r_h^4) - \frac{1}{6} B^2 - \frac{1}{2} B^2 \log r_h + \mathcal{O}(B^3), \\ T^{zz} &= r_h^4 + (r_p^4 - r_h^4) - \frac{1}{6} B^2 + \frac{1}{2} B^2 \log r_h + \mathcal{O}(B^3). \end{aligned} \quad (135)$$

To extract the energy density, pressure and magnetization, we compare (135) with the MHD formalism [43] (see Eq. 14 there). Here, we would like to point out that the AdS/CFT computations give rise to the medium contributions (denoted as $T_{F0}^{\mu\nu}$ in [43]). Consequently,

$$\varepsilon = T^{tt}, \quad p_\perp = T^{xx} = T^{yy}, \quad p_\parallel = T^{zz}. \quad (136)$$

The pressure p is identified as p_\parallel

$$p = p_\parallel = \frac{1}{2} B^2 \log r_h + \mathcal{O}(B^3) \implies 2p_{B^2} = \log r_h. \quad (137)$$

where we used the perturbative expression for r_p in (116). The magnetization M could be computed as

$$p_\perp = p_\parallel - MB \implies M = B \log r_h + \mathcal{O}(B^2). \quad (138)$$

Now we move on to the calculation of the magneto-vortical susceptibility M_Ω . In the zero magnetic field situation, we calculate M_Ω based on the following Kubo formula [33]:

$$M_\Omega = - \lim_{q_x, q_y \rightarrow 0} \frac{\langle T^{ty} J^x \rangle}{q_y q_x}. \quad (139)$$

Since M_Ω is C-odd, we need to consider the finite density RN-AdS₅ background:

$$\begin{aligned} ds^2 &= -f(r) dt^2 + \frac{dr^2}{f(r)} + r^2(dx^2 + dy^2 + dz^2), \\ V &= \left(\frac{Q}{r_h^2} - \frac{Q}{r^2} \right) dt, \quad A = 0, \end{aligned} \quad (140)$$

where

$$f(r) = r^2 \left(1 - \frac{r_h^4}{r^4} + \frac{Q^2}{3r^6} - \frac{Q^2}{3r_h^2 r^4} \right). \quad (141)$$

For consistency, we turn on the following fluctuations on top of (140):

$$\begin{aligned} \delta(ds^2) &= 2r^2 [\delta g_{tx}(r, x, y) dt dx + \delta g_{ty}(r, x, y) dt dy], \\ \delta V &= \delta V_x(r, x, y) dx + \delta V_y(r, x, y) dy. \end{aligned} \quad (142)$$

We turn attention to the Fourier space by assuming a plane wave ansatz for the fluctuations,

$$\begin{aligned} \delta g_{tx}(r, x, y) &\sim e^{iq_x x + iq_y y} \delta g_{tx}(r), \\ \delta g_{ty}(r, x, y) &\sim e^{iq_x x + iq_y y} \delta g_{ty}(r), \\ \delta V_x(r, x, y) &\sim e^{iq_x x + iq_y y} \delta V_x(r), \\ \delta V_y(r, x, y) &\sim e^{iq_x x + iq_y y} \delta V_y(r). \end{aligned} \quad (143)$$

To proceed, we collect the EOMs for the fluctuations in (142). The constraint equations $E_{rt} = 0$ and $E V^r = 0$ give rise to

$$\begin{aligned} r^{-2} f(r) \partial_r (q_x \delta g_{tx} + q_y \delta g_{ty}) \\ - \left(r^{-2} f(r) \right)' (q_x \delta g_{tx} + q_y \delta g_{ty}) = 0, \end{aligned} \quad (144)$$

$$r f(r) \partial_r (q_x \delta V_x + q_y \delta V_y) + 2Q (q_x \delta g_{tx} + q_y \delta g_{ty}) = 0. \quad (145)$$

The dynamical components of the Einstein equations $E_{tx} = E_{ty} = 0$ are

$$\partial_r(r^5 \partial_r \delta g_{tx}) + 2Q \partial_r \delta V_x + \frac{r^3}{f(r)} \times (q_x q_y \delta g_{ty} - q_y^2 \delta g_{tx}) = 0, \quad (146)$$

$$\partial_r(r^5 \partial_r \delta g_{ty}) + 2Q \partial_r \delta V_y + \frac{r^3}{f(r)} (q_x q_y \delta g_{tx} - q_x^2 \delta g_{ty}) = 0. \quad (147)$$

The dynamical components of the vector Maxwell equations $EV^x = EV^y = 0$ are

$$\partial_r[r f(r) \partial_r \delta V_x] + 2Q \partial_r \delta g_{tx} + \frac{1}{r} (q_x q_y \delta V_y - q_y^2 \delta V_x) = 0, \quad (148)$$

$$\partial_r[r f(r) \partial_r \delta V_y] + 2Q \partial_r \delta g_{ty} + \frac{1}{r} (q_x q_y \delta V_x - q_x^2 \delta V_y) = 0. \quad (149)$$

Near the AdS boundary, we impose

$$\delta V_x \xrightarrow{r \rightarrow \infty} v_x, \quad \text{others} \xrightarrow{r \rightarrow \infty} 0, \quad (150)$$

while at the horizon we have

$$\delta g_{tx}, \delta g_{ty} \xrightarrow{r \rightarrow r_h} 0, \quad \delta V_x, \delta V_y \text{ are regular at } r = r_h. \quad (151)$$

Given (139), we solve (146)–(149) in the small momenta limit. The fluctuation modes could be expanded as

$$\begin{aligned} \delta g_{tx} &= \delta g_{tx}^{(0)} + \epsilon \delta g_{tx}^{(1)} + \epsilon^2 \delta g_{tx}^{(2)}, \\ \delta g_{ty} &= \delta g_{ty}^{(0)} + \epsilon \delta g_{ty}^{(1)} + \epsilon^2 \delta g_{ty}^{(2)}, \\ \delta V_x &= \delta V_x^{(0)} + \epsilon \delta V_x^{(1)} + \epsilon^2 \delta V_x^{(2)}, \\ \delta V_y &= \delta V_y^{(0)} + \epsilon \delta V_y^{(1)} + \epsilon^2 \delta V_y^{(2)}, \end{aligned} \quad (152)$$

where $\epsilon \sim q_x, q_y$.

At the lowest order $\mathcal{O}(\epsilon^0)$, the solutions are simply given by

$$\delta V_x^{(0)} = v_x, \quad \delta g_{tx}^{(0)} = \delta g_{ty}^{(0)} = \delta V_y^{(0)} = 0. \quad (153)$$

At the first order $\mathcal{O}(\epsilon^1)$, there are no non-trivial solutions,

$$\delta g_{tx}^{(1)} = \delta g_{ty}^{(1)} = \delta V_x^{(1)} = \delta V_y^{(1)} = 0. \quad (154)$$

At the second order $\mathcal{O}(\epsilon^2)$, the equations we need are

$$\partial_r(r^5 \partial_r \delta g_{ty}^{(2)}) + 2Q \partial_r \delta V_y^{(2)} = 0, \quad (155)$$

$$\partial_r[r f(r) \partial_r \delta V_y^{(2)}] + 2Q \partial_r \delta g_{ty}^{(2)} + \frac{q_x q_y}{r} \delta V_x^{(0)} = 0. \quad (156)$$

In $\delta g_{ty}^{(2)}$, we will track the term linear in Q ($\sim \mu$) only. Therefore, the Q -term in (156) could be discarded. Furthermore, we can simply take $f(r) \rightarrow r^2(1 - r_h^4/r^4)$. Equation (156) is solved as

$$\delta V_y^{(2)} = -q_x q_y v_x \int_r^\infty \frac{\log(r_h/x)}{x^3(1 - r_h^4/x^4)} dx. \quad (157)$$

Finally, Eq. (155) is solved as

$$\delta g_{ty}^{(2)} = 2Q q_x q_y v_x \int_r^\infty \frac{dx}{x^5} \int_{r_h}^x \frac{\log(r_h/y)}{y^3(1 - r_h^4/y^4)} dy + \frac{C_0}{r^4}, \quad (158)$$

where the integration constant C_0 is fixed as

$$\begin{aligned} 2Q q_x q_y v_x \int_{r_h}^\infty \frac{dx}{x^5} \int_{r_h}^x \frac{\log(r_h/y)}{y^3(1 - r_h^4/y^4)} dy + \frac{C_0}{r_h^4} \\ = 0 \Rightarrow C_0 = \frac{\pi^2 - 8}{64r_h^2} Q q_x q_y v_x. \end{aligned} \quad (159)$$

Near the AdS boundary,

$$\delta g_{ty}^{(2)} \xrightarrow{r \rightarrow \infty} -\frac{Q q_x q_y v_x}{8r_h^2 r^4} + \mathcal{O}(r^{-5}), \quad (160)$$

which is translated to

$$T^{ty} = \frac{Q}{2r_h^2} q_x q_y v_x \Rightarrow M_\Omega = -\frac{Q}{2r_h^2} = -\frac{1}{2}\mu. \quad (161)$$

References

1. G.S. Bali, F. Bruckmann, G. Endrodi, Z. Fodor, S.D. Katz, A. Schafer, QCD quark condensate in external magnetic fields. *Phys. Rev. D* **86**, 071502 (2012). <https://doi.org/10.1103/PhysRevD.86.071502>. [arXiv:1206.4205](https://arxiv.org/abs/1206.4205) [hep-lat]
2. G.S. Bali, F. Bruckmann, G. Endrodi, Z. Fodor, S.D. Katz, S. Krieg, A. Schafer, K.K. Szabo, The QCD phase diagram for external magnetic fields. *JHEP* **02**, 044 (2012). [https://doi.org/10.1007/JHEP02\(2012\)044](https://doi.org/10.1007/JHEP02(2012)044). [arXiv:1111.4956](https://arxiv.org/abs/1111.4956) [hep-lat]
3. K.A. Mamo, Inverse magnetic catalysis in holographic models of QCD. *JHEP* **05**, 121 (2015). [https://doi.org/10.1007/JHEP05\(2015\)121](https://doi.org/10.1007/JHEP05(2015)121). [arXiv:1501.03262](https://arxiv.org/abs/1501.03262) [hep-th]
4. D. Li, M. Huang, Y. Yang, P.-H. Yuan, Inverse magnetic catalysis in the soft-wall model of AdS/QCD. *JHEP* **02**, 030 (2017). [https://doi.org/10.1007/JHEP02\(2017\)030](https://doi.org/10.1007/JHEP02(2017)030). [arXiv:1610.04618](https://arxiv.org/abs/1610.04618) [hep-th]
5. M.N. Chernodub, Spontaneous electromagnetic superconductivity of vacuum in strong magnetic field: evidence from the Nambu–Jona–Lasinio model. *Phys. Rev. Lett.* **106**, 142003 (2011). <https://doi.org/10.1103/PhysRevLett.106.142003>. [arXiv:1101.0117](https://arxiv.org/abs/1101.0117) [hep-ph]
6. M.N. Chernodub, Superconductivity of QCD vacuum in strong magnetic field. *Phys. Rev. D* **82**, 085011 (2010). <https://doi.org/10.1103/PhysRevD.82.085011>. [arXiv:1008.1055](https://arxiv.org/abs/1008.1055) [hep-ph]
7. Y. Jiang, J. Liao, Pairing phase transitions of matter under rotation. *Phys. Rev. Lett.* **117**(19), 192302 (2016). <https://doi.org/10.1103/PhysRevLett.117.192302>. [arXiv:1606.03808](https://arxiv.org/abs/1606.03808) [hep-ph]

8. S. Ebihara, K. Fukushima, K. Mameda, Boundary effects and gapped dispersion in rotating fermionic matter. *Phys. Lett. B* **764**, 94–99 (2017). <https://doi.org/10.1016/j.physletb.2016.11.010>. arXiv:1608.00336 [hep-ph]
9. A. Vilenkin, Equilibrium parity violating current in a magnetic field. *Phys. Rev. D* **22**, 3080–3084 (1980). <https://doi.org/10.1103/PhysRevD.22.3080>
10. K. Fukushima, D.E. Kharzeev, H.J. Warringa, The chiral magnetic effect. *Phys. Rev. D* **78**, 074033 (2008). <https://doi.org/10.1103/PhysRevD.78.074033>. arXiv:0808.3382 [hep-ph]
11. K. Fukushima, D.E. Kharzeev, H.J. Warringa, Real-time dynamics of the chiral magnetic effect. *Phys. Rev. Lett.* **104**, 212001 (2010). <https://doi.org/10.1103/PhysRevLett.104.212001>. arXiv:1002.2495 [hep-ph]
12. J. Erdmenger, M. Haack, M. Kaminski, A. Yarom, Fluid dynamics of R-charged black holes. *JHEP* **01**, 055 (2009). <https://doi.org/10.1088/1126-6708/2009/01/055>. arXiv:0809.2488 [hep-th]
13. N. Banerjee, J. Bhattacharya, S. Bhattacharyya, S. Dutta, R. Loganayagam, P. Surowka, Hydrodynamics from charged black branes. *JHEP* **01**, 094 (2011). [https://doi.org/10.1007/JHEP01\(2011\)094](https://doi.org/10.1007/JHEP01(2011)094). arXiv:0809.2596 [hep-th]
14. D.T. Son, P. Surowka, Hydrodynamics with triangle anomalies. *Phys. Rev. Lett.* **103**, 191601 (2009). <https://doi.org/10.1103/PhysRevLett.103.191601>. arXiv:0906.5044 [hep-th]
15. M.A. Metlitski, A.R. Zhitnitsky, Anomalous axion interactions and topological currents in dense matter. *Phys. Rev. D* **72**, 045011 (2005). <https://doi.org/10.1103/PhysRevD.72.045011>. arXiv:hep-ph/0505072
16. D.T. Son, A.R. Zhitnitsky, Quantum anomalies in dense matter. *Phys. Rev. D* **70**, 074018 (2004). <https://doi.org/10.1103/PhysRevD.70.074018>. arXiv:hep-ph/0405216
17. K. Hattori, Y. Yin, Charge redistribution from anomalous magnetovorticity coupling. *Phys. Rev. Lett.* **117**(15), 152002 (2016). <https://doi.org/10.1103/PhysRevLett.117.152002>. arXiv:1607.01513 [hep-th]
18. Y. Liu, I. Zahed, Pion condensation by rotation in a magnetic field. *Phys. Rev. Lett.* **120**(3), 032001 (2018). <https://doi.org/10.1103/PhysRevLett.120.032001>. arXiv:1711.08354 [hep-ph]
19. H.-L. Chen, K. Fukushima, X.-G. Huang, K. Mameda, Analogy between rotation and density for Dirac fermions in a magnetic field. *Phys. Rev. D* **93**(10), 104052 (2016). <https://doi.org/10.1103/PhysRevD.93.104052>. arXiv:1512.08974 [hep-ph]
20. G. Cao, L. He, Rotation induced charged pion condensation in a strong magnetic field: a Nambu–Jona–Lasino model study. *Phys. Rev. D* **100**(9), 094015 (2019). <https://doi.org/10.1103/PhysRevD.100.094015>. arXiv:1910.02728 [nucl-th]
21. H.-L. Chen, X.-G. Huang, K. Mameda, Do charged pions condense in a magnetic field with rotation? arXiv:1910.02700 [nucl-th]
22. P. Kovtun, Thermodynamics of polarized relativistic matter. *JHEP* **07**, 028 (2016). [https://doi.org/10.1007/JHEP07\(2016\)028](https://doi.org/10.1007/JHEP07(2016)028). arXiv:1606.01226 [hep-th]
23. Y. Neiman, Y. Oz, Relativistic hydrodynamics with general anomalous charges. *JHEP* **03**, 023 (2011). [https://doi.org/10.1007/JHEP03\(2011\)023](https://doi.org/10.1007/JHEP03(2011)023). arXiv:1011.5107 [hep-th]
24. K. Landsteiner, E. Megias, F. Pena-Benitez, Gravitational anomaly and transport. *Phys. Rev. Lett.* **107**, 021601 (2011). <https://doi.org/10.1103/PhysRevLett.107.021601>. arXiv:1103.5006 [hep-ph]
25. K. Landsteiner, Notes on anomaly induced transport. *Acta Phys. Polon. B* **47**, 2617 (2016). <https://doi.org/10.5506/APhysPolB.47.2617>. arXiv:1610.04413 [hep-th]
26. T.E. Clark, S.T. Love, T. ter Veldhuis, Holographic currents and Chern–Simons terms. *Phys. Rev. D* **82**, 106004 (2010). <https://doi.org/10.1103/PhysRevD.82.106004>. arXiv:1006.2400 [hep-th]
27. K. Landsteiner, E. Megias, L. Melgar, F. Pena-Benitez, Holographic gravitational anomaly and chiral vortical effect. *JHEP* **09**, 121 (2011). [https://doi.org/10.1007/JHEP09\(2011\)121](https://doi.org/10.1007/JHEP09(2011)121). arXiv:1107.0368 [hep-th]
28. S. de Haro, S.N. Solodukhin, K. Skenderis, Holographic reconstruction of space-time and renormalization in the AdS/CFT correspondence. *Commun. Math. Phys.* **217**, 595–622 (2001). <https://doi.org/10.1007/s002200100381>. arXiv:hep-th/0002230
29. B. Sahoo, H.-U. Yee, Electrified plasma in AdS/CFT correspondence. *JHEP* **11**, 095 (2010). [https://doi.org/10.1007/JHEP11\(2010\)095](https://doi.org/10.1007/JHEP11(2010)095). arXiv:1004.3541 [hep-th]
30. E. Megias, F. Pena-Benitez, Holographic gravitational anomaly in first and second order hydrodynamics. *JHEP* **05**, 115 (2013). [https://doi.org/10.1007/JHEP05\(2013\)115](https://doi.org/10.1007/JHEP05(2013)115). arXiv:1304.5529 [hep-th]
31. C. Copetti, J. Fernandez-Pendas, K. Landsteiner, E. Megias, Anomalous transport and holographic momentum relaxation. *JHEP* **09**, 004 (2017). [https://doi.org/10.1007/JHEP09\(2017\)004](https://doi.org/10.1007/JHEP09(2017)004). arXiv:1706.05294 [hep-th]
32. E. D'Hoker, P. Kraus, Magnetic brane solutions in AdS. *JHEP* **10**, 088 (2009). <https://doi.org/10.1088/1126-6708/2009/10/088>. arXiv:0908.3875 [hep-th]
33. J. Hernandez, P. Kovtun, Relativistic magnetohydrodynamics. *JHEP* **05**, 001 (2017). [https://doi.org/10.1007/JHEP05\(2017\)001](https://doi.org/10.1007/JHEP05(2017)001). arXiv:1703.08757 [hep-th]
34. J.F. Fuini, L.G. Yaffe, Far-from-equilibrium dynamics of a strongly coupled non-Abelian plasma with non-zero charge density or external magnetic field. *JHEP* **07**, 116 (2015). [https://doi.org/10.1007/JHEP07\(2015\)116](https://doi.org/10.1007/JHEP07(2015)116). arXiv:1503.07148 [hep-th]
35. A. Gynther, K. Landsteiner, F. Pena-Benitez, A. Rebhan, Holographic anomalous conductivities and the chiral magnetic effect. *JHEP* **02**, 110 (2011). [https://doi.org/10.1007/JHEP02\(2011\)110](https://doi.org/10.1007/JHEP02(2011)110). arXiv:1005.2587 [hep-th]
36. T. Tatsumi, K. Nishiyama, S. Karasawa, Novel Lifshitz point for chiral transition in the magnetic field. *Phys. Lett. B* **743**, 66–70 (2015). <https://doi.org/10.1016/j.physletb.2015.02.033>. arXiv:1405.2155 [hep-ph]
37. Y. Bu, S. Lin, Holographic magnetized chiral density wave. *Chin. Phys. C* **42**(11), 114104 (2018). <https://doi.org/10.1088/1674-1137/42/11/114104>. arXiv:1807.00330 [hep-th]
38. S. Lin, L. Yang, Mass correction to chiral vortical effect and chiral separation effect. *Phys. Rev. D* **98**(11), 114022 (2018). <https://doi.org/10.1103/PhysRevD.98.114022>. arXiv:1810.02979 [nucl-th]
39. X. Ji, Y. Liu, X.-M. Wu, Chiral vortical conductivity across a topological phase transition from holography. *Phys. Rev. D* **100**(12), 126013 (2019). <https://doi.org/10.1103/PhysRevD.100.126013>. arXiv:1904.08058 [hep-th]
40. A. Flachi, K. Fukushima, Chiral vortical effect with finite rotation, temperature, and curvature. *Phys. Rev. D* **98**(9), 096011 (2018). <https://doi.org/10.1103/PhysRevD.98.096011>. arXiv:1702.04753 [hep-th]
41. P. Kovtun, Lectures on hydrodynamic fluctuations in relativistic theories. *J. Phys. A* **45**, 473001 (2012). <https://doi.org/10.1088/1751-8113/45/47/473001>. arXiv:1205.5040 [hep-th]
42. S. Grozdanov, D.M. Hofman, N. Iqbal, Generalized global symmetries and dissipative magnetohydrodynamics. *Phys. Rev. D* **95**(9), 096003 (2017). <https://doi.org/10.1103/PhysRevD.95.096003>. arXiv:1610.07392 [hep-th]
43. X.-G. Huang, A. Sedrakian, D.H. Rischke, Kubo formulae for relativistic fluids in strong magnetic fields. *Ann. Phys.* **326**, 3075–3094 (2011). <https://doi.org/10.1016/j.aop.2011.08.001>. arXiv:1108.0602 [astro-ph.HE]
44. S.I. Finazzo, R. Critelli, R. Rougemont, and J. Noronha, Momentum transport in strongly coupled anisotropic plasmas in the presence of strong magnetic fields. *Phys. Rev. D* **94**(5), 054020 (2016). <https://doi.org/10.1103/PhysRevD.94.054020>. <https://doi.org/10.1103/PhysRevD.96.019903>. arXiv:1605.06061 [hep-ph]. [Erratum: *Phys. Rev. D* **96**(1), 019903 (2017)]

45. K. Hattori, Y. Hirono, H.-U. Yee, Y. Yin, Magneto hydrodynamics with chiral anomaly: phases of collective excitations and instabilities. *Phys. Rev. D* **100**(6), 065023 (2019). <https://doi.org/10.1103/PhysRevD.100.065023>. [arXiv:1711.08450](https://arxiv.org/abs/1711.08450) [hep-th]
46. S. Grozdanov, N. Poovuttikul, Generalised global symmetries in holography: magnetohydrodynamic waves in a strongly interacting plasma. *JHEP* **04**, 141 (2019). [arXiv:1707.04182](https://arxiv.org/abs/1707.04182) [hep-th]
47. D.M. Hofman, N. Iqbal, Generalized global symmetries and holography. *SciPost Phys.* **4**(1), 005 (2018). <https://doi.org/10.21468/SciPostPhys.4.1.005>. [arXiv:1707.08577](https://arxiv.org/abs/1707.08577) [hep-th]
48. K. Jensen, R. Loganayagam, A. Yarom, Thermodynamics, gravitational anomalies and cones. *JHEP* **02**, 088 (2013). [https://doi.org/10.1007/JHEP02\(2013\)088](https://doi.org/10.1007/JHEP02(2013)088). [arXiv:1207.5824](https://arxiv.org/abs/1207.5824) [hep-th]
49. G. Basar, D.E. Kharzeev, The Chern–Simons diffusion rate in strongly coupled N=4 SYM plasma in an external magnetic field. *Phys. Rev. D* **85**, 086012 (2012). <https://doi.org/10.1103/PhysRevD.85.086012>. [arXiv:1202.2161](https://arxiv.org/abs/1202.2161) [hep-th]